

## Review of expansive and collapsible soil volume change models within a unified elastoplastic framework

Sandra L. Houston<sup>1#</sup> , Xiong Zhang<sup>2</sup> 

Review Article

### Keywords

Volume change of unsaturated soils  
Expansive soils  
Collapsible soils  
Elastoplastic models  
Oedometer methods

### Abstract

Numerous laboratory tests on unsaturated soils revealed complex volume-change response to reduction of soil suction, resulting in early development of state surface approaches that incorporate soil expansion or collapse due to wetting under load. Nonetheless, expansive and collapsible soils are often viewed separately in research and practice, resulting in development of numerous constitutive models specific to the direction of volume change resulting from suction decrease. In addition, several elastoplastic models, developed primarily for collapse or expansion, are modified by add-on, such as multiple yield curves/surfaces, to accommodate a broader range of soil response. Current tendency to think of unsaturated soils as either expansive or collapsible (or, sometimes, stable), has likely contributed to lack of development of a unified approach to unsaturated soil volume change. In this paper, common research and practice approaches to volume change of unsaturated soils are reviewed within a simple macro-level elastoplastic framework, the Modified State Surface Approach (MSSA). The MSSA emerges as a unifying approach that accommodates complex volume change response of unsaturated soil, whether the soil exhibits collapse, expansion, or both. Suggestions are made for minor adjustments to existing constitutive models from this review, typically resulting in simplification and/or benefit to some of the most-used constitutive models for unsaturated soil volume change. In the review of practice-based approaches, the surrogate path method (SPM), an oedometer/suction-based approach, is demonstrated to be consistent with the MSSA framework, broadly applicable for use with expansive and collapsible soils, and yielding results consistent with measured field stress-path soil response.

## 1. Introduction

An unsaturated soil exhibits volume change in response to changes in one or both stress state variables (net total stress and matric suction). For unsaturated soil volume change, changes in volume of the soil matrix and the water phase (commonly represented by the void ratio and gravimetric water content, respectively) occur, giving rise to well-known state surfaces in unsaturated soil mechanics (Matyas & Radhakrishna, 1968; Fredlund & Morgenstern, 1976, 1977; Lloret & Alonso, 1980, 1985). Figure 1 shows a representative schematic plot of the void ratio surface of Matyas & Radhakrishna (1968). As discussed in Wheeler & Karube (1996), volume change response of unsaturated soils is complex, particularly for changes in soil suction. An increase in net total stress always results in volume reduction of an unsaturated soil (AB or A'B' in Figure 1). However, essentially any soil with some clay content may compress or

expand in response to reduction of soil suction, depending on the magnitude of the net total stress and the initial soil suction, as well as soil structure (Jennings & Burland, 1962; Fredlund & Rahardjo, 1993; Delage & Graham, 1996; White, 2007). At low net total stress, a clay typically exhibits expansion upon wetting (AA' as shown in Figure 1a), but at high net total stress, it may exhibit compression upon wetting (BB' as shown in Figure 1). Computation of volume change requires the consideration of the initial soil state, including stress history, along with simultaneous consideration of both stress state variables of net total stress and matric suction. Thus, it can be difficult to intuit even the direction (compression or expansion) of suction-induced volume change.

Historically, geotechnical engineers have classified a soil that exhibits substantial increases in volume in response to wetting as expansive and soil that exhibits substantial

<sup>#</sup>Corresponding author. E-mail address: sandra.houston@asu.edu

<sup>1</sup>Arizona State University, Tempe, AZ, USA.

<sup>2</sup>Missouri University of Science and Technology, Rolla, MO, USA.

Submitted on March 11, 2021; Final Acceptance on June 16, 2021; Discussion open until November 30, 2021.

<https://doi.org/10.28927/SR.2021.064321>



This is an Open Access article distributed under the terms of the Creative Commons Attribution License, which permits unrestricted use, distribution, and reproduction in any medium, provided the original work is properly cited.

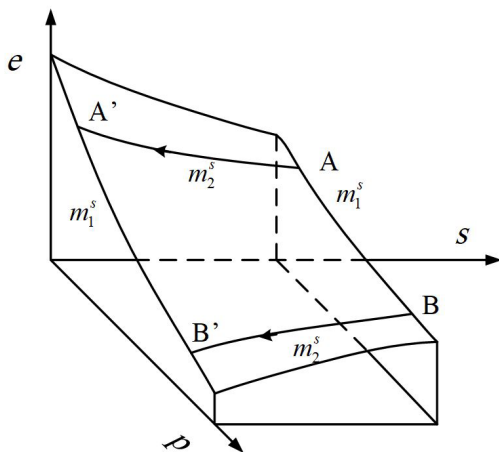


**Figure 1.** Warped state surfaces for void ratio of Matyas & Radhakrishna (1968), showing instantaneous state surface slopes with respect to matric suction and net total stress of Fredlund & Rahardjo (1993).

decreases in volume in response to wetting as collapsible. Such classifications are convenient short hands, as are other common generalizations – unsaturated fat clays increase in volume when wetted whereas unsaturated low-density silts decrease in volume when wetted; smectite clays of sedimentary origin expand upon wetting, and loessial soils collapse upon wetting. Further, expansive clays and collapsible soils, separately rather than together, are classified as natural hazards due to the potential for severe damage to infrastructure that can occur when soils exhibit large volume change upon wetting under load. Expansive soils result in an estimated \$15 billion annual cost of damage to infrastructure in the USA, more than £400 million a year in cost to British insurance companies, and are recognized as one of the most common causes of damage to roadways (Driscoll & Crilly, 2000; Jones, 2018; Jones & Jefferson, 2012; Nelson & Miller, 1992; Dessouky et al., 2012). Collapsible soils can cause severe damage to critical infrastructure, including canals, dams, pipelines, roads, and buildings (Knodel, 1992; Li et al., 2016; Fonte et al., 2017).

The long history of separation of expansive soil and collapsible soils in research and practice has resulted in the creation of many volume change constitutive models that are specific to the direction of volume change upon soil wetting (suction reduction). Some elastoplastic models are primarily for collapsible or expansive conditions, but empirically, and often inconsistently, incorporate multiple yield surfaces to accommodate both volume change responses. A constitutive model for evaluation of volume change of an expansive clay may not be best for predominantly collapsible soils and vice versa. This reality of emphasis on either expansive or collapsible response has not necessarily hampered progress in dealing with real-world unsaturated soil volume-change problems. But separation of expansive and collapsible soils has contributed, most likely, to lack of progress in the

development of a unified approach to calculation of volume change of unsaturated soils, which can lead to significant differences in volume change prediction, even for a specific field prototype.

More general volume change models are appropriate for heterogeneous soil profiles containing soil types with mixed (expansion or collapse) suction-changed induced volume change response, and to more homogenous soil profiles that exhibit both expansion and collapse upon wetting, depending on the net total stress conditions. It is the intent of this paper to briefly review available approaches to modeling expansive and collapsible soils and to present in more detail the modified state surface approach (MSSA), as a broadly applicable macro-level elastoplastic framework for modeling unsaturated soil volume change.

The MSSA, first introduced by Zhang & Lytton (2009a, b), allows for a soil response of expansion, collapse, or both and accommodates the full range of volume change response through the use of unique elastoplastic state surfaces for void ratio and water content. The MSSA is based on two independent stress state variables of matric suction and mean net stress and builds upon the traditional state surface approach (Matyas & Radhakrishna, 1968; Lloret & Alonso, 1980, 1985; Fredlund & Rahardjo, 1993). The MSSA was later extended to handle triaxial stress state conditions (Zhang, 2010), and coupled hydro-mechanical unsaturated soil behavior (Zhang & Lytton, 2012), with considerations of both mechanical and hydraulic hysteresis (Riad & Zhang, 2020, 2021). However, in this paper, only soil structure (void ratio) volume change constitutive models are considered, and companion volume change models for the water phase are not addressed. It will be demonstrated how existing approaches to modeling unsaturated soil volume change can be accommodated within the MSSA framework. Where minor adjustments to existing constitutive models are shown to be appropriate, according to the MSSA, such modifications will be shown to lead to overall simplification and some benefits, in general, in the constitutive modelling of unsaturated soils.

## 2. Overview of available constitutive models

Decades of research on expansive and collapsible soils has resulted in the development of numerous constitutive models for the estimation of volume change of unsaturated soils. Foundation engineering work resulted in practice-based models for the computation of vertical strains (deformations), under  $K_0$  conditions: (a) for expansive soils (Washington, 1983; Picornell & Lytton, 1984; Lytton, 1977; Fredlund et al., 1980; Nelson & Miller, 1992; Noorany & Houston, 1995; Overton et al., 2006; Adem & Vanapalli, 2013; Houston & Houston, 2018), and (b) for collapsible soils (Jennings & Knight, 1957; Houston et al., 1988; Washington, 1983; Barden et al., 1973; Houston & Houston, 1997). Many 1-D models are for problems of either expansion or collapse volume change due to monotonic suction change (typically

wetting) under constant confining stress (load), due to the importance of this boundary condition for many practical problems. A suction-oedometer method, termed the surrogate path method (SPM), is applicable to expansive and collapsible soils, and is a practice-based approach for estimation of 1-D volume change of unsaturated soil for monotonic change in soil suction under constant net total stress conditions (Houston & Houston, 2018; Singhal, 2010).

Fredlund & Rahardjo (1993) and Fredlund & Morgenstern (1976) set forth a general 3-D volume change model for unsaturated soils based on incremental elasticity, which was expanded upon by Vu & Fredlund (2004, 2006) in the analysis of wetting-induced expansive soil movements. Zhang (2005), Wray et al. (2005), and Zhang & Briaud (2015) also developed generalized 3-D volume change models for expansive soils based on incremental elasticity. Theoretically, both expansive and collapsible soil response can be modeled using incremental elasticity due to the ability to adjust soil parameters for various ranges in a stress state. However, unsaturated collapsible soils exhibit clear irrecoverable volume change, and the process is therefore truly elastoplastic (Alonso, 1987; Alonso et al., 1990). The emphasis to date has been on the use of incremental 3-D elastic models for problems of soil expansion, with few exceptions such as Lloret & Alonso (1980) and Pereira & Fredlund (1997) who used incremental elasticity for collapsible soils.

Several elastoplastic models using the two stress state variable approach for the estimation of volume change of unsaturated soils are available (Alonso et al., 1990, 1994, 1999; Gens & Alonso, 1992; Cui & Delage, 1996; Bolzon et al., 1996; Delage & Graham, 1996; Gens et al., 1996; Wheeler & Sivakumar, 1995; Wheeler, 1996; Wheeler et al., 2003; Dangla et al., 1997; Vaunat et al., 2000; Geiser et al., 2000; Khalili & Loret, 2001; Gallipoli et al., 2003a, b; Sheng et al., 2003a, b, 2004, 2008a, b; Tamagnini, 2004; Vassallo, et al., 2007; Costa & Alonso, 2009). The focus of early elastoplastic models was on unsaturated collapsible soil behavior due to the vast attention placed on the Barcelona Basic Model, BBM (Alonso et al., 1990). Within the BBM, soil expansion is typically accomplished through the introduction of an additional Suction Increase (SI) yield surface. While the use of multiple yield surfaces accomplishes the goal of well-matching laboratory test results, this approach often results in sharp transitions in soil response at the intersections of the yield surfaces, and some inconsistencies between the constitutive model and established virgin loading response of soils (Delage & Graham, 1996; Zhang & Lytton, 2009a, b). Zhang & Lytton (2009a, b) present a macro-level elastoplastic method, the modified state surface approach (MSSA), which makes use of a unique virgin loading state surface. The MSSA is theoretically applicable to both collapsible and expansive soils.

Alonso et al. (1999) proposed an elastoplastic constitutive model (BExM), incorporating soil responses at both the micro- and macro-levels to simulate wetting-induced swell of expansive soils, again making use of multiple

yield surfaces. Several other dual structure (micro-macro) constitutive models have been developed for expansive soils (e.g., Sánchez et al., 2005; Vilarrasa et al., 2016). Micro-macro constitutive models for collapsible soils, however, have not received a great deal of attention to date. Highly complex thermo-hydro-mechanical models have been developed, particularly for expansive soils, and mainly due to consideration of using clay-bentonite soil mixtures as part of a barrier system in the containment of radioactive wastes (Gens & Olivella, 2001; Lloret et al., 2003; Sánchez et al., 2005). At the research level, micro-macro constitutive models appear to play an important role, most notably in applications to nuclear waste isolation. On the other hand, dual-structure/micro-macro constitutive models require the determination of many parameters, too many of which can be obtained only by estimation from back-analysis, rather than by direct determination. Complex micro-macro models can also represent a deterrent to the application of unsaturated soil mechanics to routine geotechnical engineering problems.

Unsaturated soil volume change constitutive models may be macro-level or micro-macro level in nature. The micro-level structure of common expansive clay minerals allows firm absorption of water internal to particles, increasing the spacing between particles, and inducing swell macroscopically (Lin & Cerato, 2014; Sánchez et al., 2005). In collapsible soils, the water leads to the softening of clay particles that bind the open-void macro-structure of the soil together, contributing to the triggering of collapse (Liu et al., 2016). An understanding of the role of micro-level response to changes in the state of stress of unsaturated soil is important and can be particularly useful in the search and for selection of mitigation alternatives, and micro-level investigations lead to enhanced understanding of the role of water as a volume-change trigger (Bellil et al., 2018; Liu et al., 2016; Lin et al., 2013). However, it can be debated whether modeling of micro-level phenomena is required, or desirable, in the computation volume change of unsaturated soils (Vilarrasa et al., 2016; Alonso et al., 1999; Fredlund & Morgenstern, 1976; Fredlund, 1979; Houston, 2019).

Relatively simple macro-level approaches, requiring experimentally obtainable soil parameters, are available for the computation of volume change of unsaturated soils, whether the response is expansion or collapse, or both, as cited above. Such models may be based on coupled or uncoupled hydro-mechanical approaches, and may be 3-D incremental elastic or elastoplastic, or simply limited to 1-D monotonic loading conditions. An argument can be made for the use of the simplest appropriate model for the particular volume change case at hand. The MSSA, as first proposed by Zhang & Lytton (2009a, b, 2012) for isotropic conditions and then extended to triaxial stress states (Zhang, 2010; Zhang et al., 2016a) with consideration of coupled hydro-mechanical hysteresis (Riad & Zhang, 2020, 2021), is a generalized elastoplastic framework that is theoretically sound and generally appropriate across all known unsaturated

soil volume change responses. The MSSA is not a specific constitutive model itself but can be viewed as a unifying framework to study existing models and develop new models for unsaturated soils.

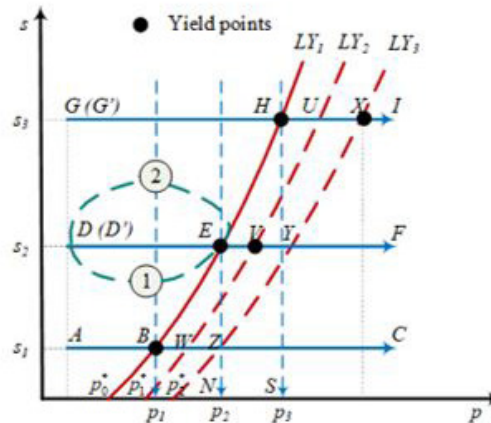
### 3. Modified state surface approach

Conventional elasto-plastic models for soils are developed in an incremental form according to classical elastoplasticity, which was first applied to solid materials such as metals. The use of simple stress-strain relationships, while convenient and straightforward where laboratory data is uncomplicated, is not particularly helpful for unsaturated soils where behavior is highly nonlinear and laboratory results have to be compared from multiple specimens with differing stress histories, and where multiple stress state variables influence the soil responses. In the development of commonly used unsaturated soil elastoplastic models, some of the inherent relationships between different components of the model have not been clearly explained in the past. In addition, unsaturated soil elastoplastic models have not taken full advantage of some features of material behavior, such as the uniqueness of the state boundary surface for virgin loading conditions. Due to unsaturated soil response being highly nonlinear and influenced by multiple factors, when the incremental form for elastoplastic behavior is used, huge challenges are created for the testing, constitutive model development and model calibration (D’Onza et al., 2015). By contrast, the MSSA takes full advantage of the uniqueness of the state boundary surface (elastoplastic virgin loading surface), simplifying the process of constitutive modeling. The MSSA can be used to deal with large amounts of potentially confusing data and synthesize the data into a usable form. The MSSA can be used to explain the elastoplastic behavior of unsaturated soils in a relatively simple way without undue complication.

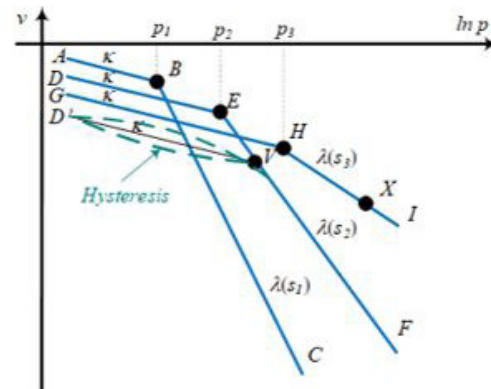
#### 3.1 Principle of the MSSA

The principle of the MSSA can be illustrated by Figure 2. Figure 2 shows the stress paths for three isotropic loading-unloading-reloading tests. Under an arbitrary constant suction  $s = s_2$ , the soil specimen has an initial condition of point D. The initial yield curve of the soil is  $LY_1$  with a preconsolidation stress of  $p_0^*$  at  $s = 0$  kPa and the yield stress at  $s = s_2$  is  $p_2$  at point E (Figure 2b). The soil is loaded from D to E to V, unloaded from V to D’, and then reloaded from D’ to V to F in Figure 2b which illustrates a typical soil response in the  $v-\ln p$  plane when the hysteresis is neglected. The following observations can be made from the process:

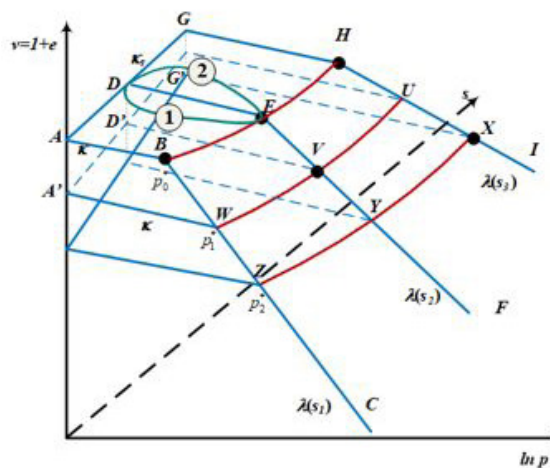
1. Regardless of stress path and stress history, the shape and position of the virgin loading curve EVF are always the same for the soil in the  $v-\ln p$  plane. Plastic loading only changes the range of the virgin



(a)



(b)



(c)

**Figure 2.** Principle of the MSSA. (a) conventional interpretation of tests to determine parameters for the BBM (Alonso et al., 1990); (b) volume change upon loading at different suctions from suction controlled compression tests; (c) three-dimensional representation of volume change of the soil.

loading curve. For example, the initial virgin loading curve for the soil is EVF. After loading from D to E to V, the virgin curve for the soil is VF;

2. During an elastic loading or unloading process, for example, from D to E, from V to D', or from D' to V, the shape and position of the unloading-reloading curve remain unchanged in the  $v\text{-ln}p$  plane. During a plastic loading process, the shape and slope of the unloading-reloading curve remains unchanged in the  $v\text{-ln}p$  plane, but its position will change. Specifically, the unloading-reloading curve will move downward in parallel with the original unloading-reloading curve. The range of the elastic zone also expands due to the increase in the preconsolidation stress from  $p_1$  to  $p_1^*$ ;
3. The yield point V is the intersection of the unloading-reloading curve and the virgin loading curve for  $s = s_2$ .

It is worth noting that in nearly all existing constitutive models  $\kappa$  is assumed a constant. To keep the explanation simple,  $\kappa$  is assumed a constant in the following discussion. This assumption can be easily taken out in the use of the MSSA to handle more general cases of varying  $\kappa$ .

Consider two other stress paths from D to E, i.e. paths 1 and 2 as shown in Figure 2a, and in the elastic zone. Since stress paths 1 and 2 are in the elastic zone, the specific volume changes are stress path independent. The results obtained for the two stress paths should be the same and the volume in the elastic zone can be expressed as a surface ABEHGDA in the  $v\text{-}p\text{-}s$  space as shown in Figure 2c (Zhang & Lytton, 2009a, b).

Figure 2c shows the specific volume change for the stress paths in Figure 2a in the  $v\text{-}p\text{-}s$  space. All the elastic volume changes, such as stress paths 1 and 2 and DE are on the same surface of ABEHGDA. When there is a plastic loading, similar to the previous discussion, the shape and position of the virgin loading curve EVF are always the same in the  $v\text{-}p\text{-}s$  space regardless of the previous stress path and stress history in the elastic zone. It can also be proven that when there is unloading, any unloading stress path must fall on a lower elastic surface.

Compression tests can be performed at any arbitrary suction level, such as  $s_1$  and  $s_3$  as shown in Figures 2a and 2b. Consequently, the virgin curves at different suction levels as shown in Figure 2b will form a "plastic (virgin) loading surface" in the  $v\text{-}p\text{-}s$  space such as BEHUXYZWB in Figure 2c. The location and shape of the plastic surface will always remain the same in the  $v\text{-}p\text{-}s$  space and the plastic surface is unique. The uniqueness of the virgin state boundary surface is a fundamental assumption made in the constitutive modeling of elastoplastic soil behavior. The uniqueness of the state boundary surface for unsaturated soils has been experimentally verified by Wheeler & Sivakumar (1995). The plastic surface BEHUXYZWB in Figure 2c is the shape of the state boundary surface for isotropic conditions. In the

$v\text{-}p\text{-}s$  space, the following assertions can be made for the elastic and plastic surfaces:

1. The shape and position of the plastic surface are always the same for the soil in the  $v\text{-}p\text{-}s$  space. Virgin loading only changes the range of the plastic surface;
2. During an elastic loading or unloading process, the shape and position of the unloading-reloading elastic surface and the plastic surface remain unchanged in the  $v\text{-}p\text{-}s$  space. The specific volume of any isotropic elastic loading or unloading stress path must fall on the elastic surface in the  $v\text{-}p\text{-}s$  space. During a plastic loading process, the shape of the unloading-reloading elastic surface remains unchanged ( $\kappa$  and  $\kappa_c$  are constants for an assumed planar elastic surface), but its position will shift. Specifically, the unloading-reloading elastic surface will move downward in parallel with the original unloading-reloading elastic surface. For example, the unloading stress path V to D' will fall on the new elastic surface A'WVUG'D'. The volume change of any isotropic plastic loading stress path must fall on the plastic surface in the  $v\text{-}p\text{-}s$  space;
3. The yield curve is the intersection of the unloading-reloading elastic surface and the plastic surface.

The MSSA can be easily extended to the triaxial stress states in the  $v\text{-}p\text{-}q\text{-}s$  space (which also considers deviator stress,  $q$ ) as follows (Zhang, 2010; Zhang et al., 2016a, b):

1. There is a unique state boundary surface in the elastoplastic region which is always unchanged in the  $v\text{-}p\text{-}q\text{-}s$  space;
2. The elastic surface is movable, but only moves when there is plastic loading. The elastic surface is fixed when there is elastic loading or unloading;
3. All the soil responses will fall on either the elastic or plastic surface;
4. The intersection between the elastic and plastic hypersurface is the yield surface; and
5. The plastic hypersurface ends when the soil fails, which is at the critical state.

Zhang & Lytton (2012) extended the MSSA for the coupled hydro-mechanical behavior of unsaturated soils. Riad & Zhang (2020, 2021) further extended the MSSA to include the coupled hydro-mechanical hysteresis for unsaturated soils. However, here only the soil structure constitutive relationships are discussed.

### 3.2 Surfaces used in the BBM

The MSSA can be used to explain existing constitutive models in a simple way. As an example, Zhang & Lytton (2009a) derived the close-form expressions of the elastic and elastoplastic surfaces for the BBM (Equations 1, 2, and 3, below) and successfully used the MSSA to represent many unsaturated soil behaviors, including the stress path independency under isotropic conditions. Figure 3 shows the

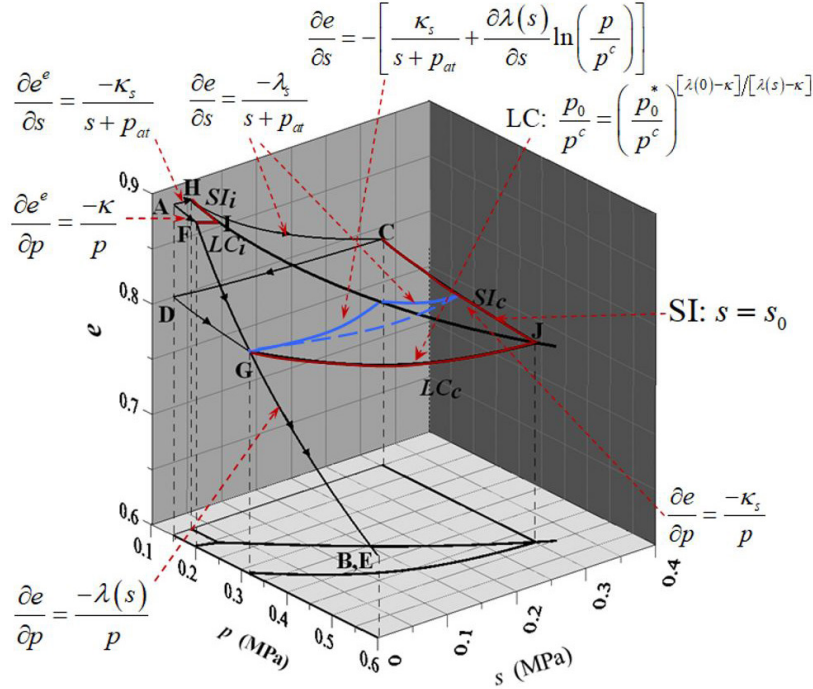


**Figure 3.** State Boundary Surface for the BBM (modified from Zhang & Lytton, 2009a).

elastic and plastic surfaces used in the BBM. They include an elastic surface AFIH and the plastic surface which is made up of two parts: a plastic collapsible surface FIJG (corresponding to the LC yield curve) and a plastic expansive surface HIJC (corresponding to the SI curve). The mathematical expressions for the three surfaces are as follows:

$$e^e = C_1 - \kappa \ln p - \kappa_s \ln(s + p_{at}) \quad (1)$$

(elastic surface AFIH)

$$e = C_2 - \kappa_s \ln\left(\frac{s + p_{at}}{p_{at}}\right) - \lambda(s) \ln\left(\frac{p}{p^c}\right) \quad (2)$$

(plastic collapsible surface FIJG)

$$e = C_3 - \kappa \ln p - \lambda_s \ln(s + p_{at}) \quad (3)$$

(plastic expansive surface HIJC)

where  $\lambda(s) = \lambda(0)[(1-r)\exp(-\beta s) + r]$ ,  $r$  = parameter controlling the slope of the virgin compression line,  $\beta$  = parameter controlling the slope of the virgin compression line for  $s \neq 0$ ,  $\lambda(0)$  = slope of the virgin compression line associated with the mean net stress at saturation ( $s=0$ );  $p^c$  = reference stress,  $C_2 = N(0)$  in the BBM = a constant,  $\lambda_s$  = slope of the virgin compression line associated with soil suction,  $p_{at}$  = atmospheric pressure,  $\kappa$  = slope of the unloading-reloading line associated to the mean net stress,  $\kappa_s$  = slope of the unloading-reloading line associated with soil suction, and  $C_1$  and  $C_3$  = are constants. The superscripts “e” represents the elastic change in the specific volume.

The LC yield curve is the intersection of the elastic surface and collapsible soil surface. In other words, the points on the LC curve must simultaneously satisfy Equations 1 and 2, which gives:

$$\ln\left(\frac{p}{p^c}\right) = \frac{C_4}{\lambda(s) - \kappa} \quad (4)$$

where  $C_4 = N(0) - C_1 + \kappa \ln(p^c) + \kappa_s \ln(p_{at})$  = constant. The yield stress when the soil is saturated is the preconsolidation stress, that is,  $p = p_0^*$  when  $s = 0$ , which gives:

$$C_4 = [\lambda(0) - \kappa] \ln\left(\frac{p_0^*}{p^c}\right) \quad (5)$$

Substituting Equation 4 into Equation 3, the yield curve equation in the BBM is obtained as follows:

$$p = p^c \left[ \frac{p_0^*}{p^c} \right]^{\frac{\lambda(0) - \kappa}{\lambda(s) - \kappa}} \quad (6)$$

Similarly, the SI yield curve is the intersection of the elastic surface and the plastic expansive soil surface. The points on the SI curve must simultaneously satisfy Equations 1 and 3 as expressed as follows.

$$s = e^{\frac{C_3 - C_1}{(\lambda_s - \kappa_s)}} - p_{at} = \text{constant} \quad (7)$$

Zhang (2010) also derived the plastic hardening equation for the BBM under a triaxial stress states as follows:

$$e = C_2 - \kappa \ln \frac{p}{p^c} - \kappa_s \ln \left( \frac{s + p_{at}}{p_{at}} \right) - (\lambda(s) - \kappa) \left[ \ln \left( p + \frac{q^2}{M^2(p + ks)} \right) - \ln p^c \right] \quad (8)$$

where  $q = \sigma_1 - \sigma_3 =$  deviatoric stress,  $k =$  parameter that relates cohesion and suction, and  $M =$  slope of theoretical critical state line.

The above equations, and Figure 3, show the BBM model within the framework of the MSSA. The BBM was selected as an example to demonstrate how the MSSA principles can be used in describing existing elastoplastic models. Similarly, other elastoplastic models for unsaturated soils can be described within the MSSA framework, provided that the model maintains consistency with all of the requirements of traditional elastoplastic theory.

### 3.3 Relationship between MSSA and existing approaches

The MSSA is consistent with the existing theories of elastoplasticity for unsaturated soils. At present, most researchers first propose some constitutive relationships for specific soil behavior in the elastic and elastoplastic zones in incremental forms and then the constitutive relationships are assembled together into a constitutive model to predict soil behavior under arbitrary stress paths. For example, in the BBM, in the elastic zone, incremental formulations were developed to calculate the specific volume changes for an unsaturated soil due to net total stress and suction as follows:

$$\frac{\partial e^e}{\partial p} = \frac{-\kappa}{p} \quad (9)$$

$$\frac{\partial e^e}{\partial s} = \frac{-\kappa_s}{s + p_{at}} \quad (10)$$

Figure 3 also shows the partial derivatives of the BBM surfaces with respect to the net total stress and matric suction. When there are simultaneous changes in the net total stress and suction in the elastic region, the above two equations are assembled together to calculate the total void ratio change:

$$de^e = -\kappa \frac{dp}{p} - \kappa_s \frac{ds}{s + p_{at}} \quad (11)$$

The specific volume change from a known initial point to any stress state in the elastic region is the line integral of Equation 11, resulting in Equation 1. Equation 1 is the closed form expression for void ratio for the elastic surface of the BBM, which was obtained using the MSSA. When the constitutive relations are simple linear equations, the level of difficulty in using the MSSA and the conventional incremental formulation is about the same. Equations 9 and

10 can be obtained by taking partial derivatives of Equation 1 with respect to the net total stress and suction respectively, demonstrating that the incremental plasticity and MSSA methods are interchangeable.

Unsaturated soil behavior, however, is very complicated and notoriously highly nonlinear. It is hence very difficult to use the incremental approach to develop constitutive models for unsaturated soils. For example, use of the incremental formulation to develop the BBM under isotropic conditions requires the following two constitutive relations to describe the plastic collapsible surface (FIJG as shown in Figure 3, corresponding to the LC yield curve) in the original BBM:

$$\frac{\partial e}{\partial p} = \frac{-\lambda(s)}{p} \quad (12)$$

$$\frac{\partial e}{\partial s} = - \left[ \frac{\kappa_s}{s + p_{at}} + \frac{\partial \lambda(s)}{\partial s} \ln \left( \frac{p}{p^s} \right) \right] \quad (13)$$

While Equation 12 is simple and frequently adopted by most researchers, Equation 13 is very complicated and difficult to visualize, or even imagine. In addition, Equations 12 and 13 are interdependent (Zhang & Lytton, 2008). In the original BBM, such a complicated formulation was successfully avoided by properly selecting  $\lambda(s)$  and  $N(s)$  in integrated forms. However, such clever approaches to simplification are not commonly used for constitutive modelling of unsaturated soils.

Similarly, the following two constitutive relations to describe the plastic expansive soil surface (corresponding to the SI yield curve) in the original BBM:

$$\frac{\partial e}{\partial p} = \frac{-\kappa}{p} \quad (14)$$

$$\frac{\partial e}{\partial s} = - \frac{\lambda_s}{s + p_{at}} \quad (15)$$

Equation 14 is the same as Equation 9, which is caused by the assumed horizontal SI yield curve. Equations 13 and 15 are significantly different and are used to simulate the collapse and swelling upon wetting for unsaturated soils, respectively. More detailed comparison and explanation regarding Equations 12 to 15 will be made in the later sections.

Another simple example of challenges faced in use of incremental formulations can be made by introducing some dependency on suction in Equation 9 in elastic region, such as in Equation 16:

$$\frac{\partial e^e}{\partial p} = \frac{-\kappa}{p + s} \quad (16)$$

Equation 16 violates stress path independency in the elastic region, simply from the addition of suction in Equation 9. In the plot of Figure 2, Equations 9 and 10 are

used to describe the elastic surface, and taking two different paths, 1 and 2, in the elastic region results in arrival at the same void ratio, point E (Figure 2). However, if Equation 16 is adopted to replace Equation 9, the two different elastic region stress paths of 1 and 2 of Figure 2 will no longer give the same void ratio at point E within the in  $p$ - $s$ - $v$  space of Figure 2c. This directly conflicts with the elasticity assumption in the elastic region, as mentioned by Wheeler & Karube (1996), but received little attention. The conflict with required stress path independency in the elastic zone is due to failure to adhere to Green's theorem, as discussed in detail by Zhang & Lytton (2008).

As can be seen, use of the incremental formulation approach makes it very difficult for constitutive modeling of highly nonlinear unsaturated soil behavior. Similar discussions have been provided by Zhang & Lytton (2008) regarding the SFG model (Sheng et al., 2008a). Instead, if the MSSA is used, one just needs to obtain the best-fit smooth functions for the elastic and plastic surfaces, matching the results from available isotropic compression tests. In this way, the constitutive model for isotropic conditions is obtained as well as the yield curve and its evolution with plastic hardening (Zhang et al., 2010; Zhang, 2016). After that, by simply taking partial derivatives of the elastic and elastoplastic surfaces, the incremental formulation of the elastoplastic model is obtained in a consistent way. Using the MSSA, there is no need to check consistency with laboratory/observed soil response since Green's theorem is automatically satisfied. When incremental formulations are used, consistency with observed soil response is not automatically assured, which can lead to violation of fundamentals of elastoplastic theory as discussed in the previous sections.

The MSSA can be used to describe some existing models within a unified framework, and also to develop new models. Zhang & Lytton (2009a) indicated that for the same experimental results of Karube (1986), the MSSA can be used to develop a simpler model compared to the BBM (6 model parameters in the MSSA model vs. 11 in the BBM). Also, for the specific Karube (1986) data, the MSSA predictions represent an improvement over those obtained using the BBM (Alonso et al. 1990).

### 3.4 Determination of yield curve and model development

An alternative way to develop a constitutive model using an incremental formulation is to define the elastic relationship and the yield curve and its evolution. As pointed out by Wheeler & Karube (1996, p. 1338), "[...] *in developing an elastoplastic model, it is therefore only necessary to define either the changing shape of the yield curve as it expands or the form of the normal compression lines for different values of suction.*" This approach is relatively straightforward and well-established for both saturated and unsaturated soils.

However, it is very difficult to accurately determine the yield curve and its evolution, as demonstrated below.

It was extensively accepted that the shape of the BBM LC yield curve can be independently determined from isotropic loading tests at varying constant suction using soil specimens with identical stress histories (Alonso et al., 1990, 1994, 1999; Gens & Alonso, 1992; Delage & Graham, 1996; Gens et al., 1996; Wheeler & Karube, 1996; Cui & Delage, 1996; Wheeler & Sivakumar, 1995; Vaunat et al., 2000; Robles & Elorza, 2002; Gallipoli et al., 2003a; Sheng et al., 2004; Wheeler, 1996; Wheeler et al., 2003; Thu et al., 2007). Figure 2a schematically illustrates the stress paths for three isotropic loading tests. Figure 2b shows the specific volume  $v$  versus  $\ln p$  curves for three isotropic loading tests under constant suction. The three yield points, determined by Casagrande's method (Casagrande, 1936) for each test, are B, E, and H, respectively, as shown in Figure 2b. These points are connected into a curve in Figure 2a to represent the initial shape of the BBM LC yield curve for the soil.

Although the above method is straightforward and well-established, it is difficult to implement correctly in the laboratory since it requires that all tested soil specimens have exactly identical stress histories. However, identical specimen history is only theoretically possible because loading, drying, and wetting can cause the soil to yield and the positions of the SI yield curves to change. In addition, even if identical specimens can be obtained, the soil may have different stress histories due to improper experimental design resulting from the initial positions of the LC and SI yield curves being unknown before the soil specimens are tested (Zhang et al., 2010). Numerous researchers reported that carefully prepared "identical specimens" were found to have different yield points when the soil specimens were tested following exact stress paths (Wheeler & Sivakumar, 1995; Rampino et al., 2000; Blatz & Graham, 2003). For soil specimens with different stress histories, their positions of LC and SI yield curves will be different. Furthermore, the Casagrande's method is an empirical method and cannot produce highly accurate results for the yield stress. Consequently, use of the above conventional method for obtaining the LC yield curve can lead to incorrect results.

Consider the MSSA principles represented in Figure 2, when the soil specimens have different stress histories, or the stress histories are changed during the soil preparation process, the actual test results could be D'V YF and G'XI in Figure 2c for the stress paths D'V YF and G'XI in Figure 2a. Since the patterns of the results for stress paths with different stress histories are very similar, such as DEVF and D'VF in Figure 2b, one can easily mistake yield point V as E and consider BVX as the shape of the yield curve, when in fact the point V belongs to another yield curve (UVW) different from the actual yield curve of BEH. It is noted that there are many other possibilities for the relative positions of the yield points, and therefore use of conventional methods for determination of the LC curve can result in yield curves with

shapes significantly different from either BVX or BEH. In addition, the above approach can only be used to estimate the initial shape of the yield curve. Typically only one yield curve is experimentally determined from three or more suction-controlled laboratory compression tests for each LC determination, and data on how the yield curve evolves during the plastic hardening process is often unavailable.

One important application of the MSSA is to determine the shape of yield curves and their evolution, as discussed in Zhang et al. (2010). The MSSA clearly defines the relationship between the form of the normal compression lines in the  $v: p$  plane and the shape of the yield curve as it expands in the  $s: p$  plane. According to MSSA, the yield curves are the intersection of the elastic and plastic surfaces. The evolution of the yield curves forms the plastic surface or, one can say that the plastic surface is a “trace” of the yield curves. Consider the case where three suction-controlled compression test specimens do not have the same stress history. In this case, results from the three isotropic compression tests could, for example, be ABC, D’VF, and G’XI as shown in Figure 2c, resulting in determination of three yield points B, V, and X, belonging to three different yield curves,  $LY_1$ ,  $LY_2$ , and  $LY_3$  (Figure 2a) respectively. As can be seen in Figure 2c, in the three-dimensional  $p-s-v$  plot the virgin normal compression curves BC, VF, and XI will fall on a unique plastic hardening surface while the elastic compression curves AB, D’V, and G’X belong to different elastic surfaces. According to the MSSA, the shape and position of the elastoplastic surface does not change during yielding (but the range of the plastic hardening surface will change). Consequently, the plastic hardening surface obtained from the three soil specimens with different stress histories, BCFIXV, is a subset of the plastic hardening surface that formed from the three theoretical soil specimens with the exactly the same stress history (BCFIHE). Using the principles of the MSSA, the virgin compression curves BC, VF, and XI establish the shape of the plastic surface, in spite of the use of non-identical soil specimens in the laboratory testing. The elastic surface (under an assumption of planar shape) is established by the constants  $\kappa$  and  $\kappa_c$  obtained from the laboratory compression tests. As long as the shape of the elastic and elastoplastic surfaces is well-fit by smooth functions, the shape of the yield curve is determined, and its evolution is established by a parallel shift of the elastic surface downward.

Use of the MSSA to obtain shapes of the yield surface and elastic surface does not require precise determination of the yield stress. If one is not certain whether the determined yield stress is accurate, an arbitrarily larger yield stress can be assumed, and the shape of the plastic surface will not be influenced. For example, Figure 4 compares the LC and SI yield curves obtained by Thu et al. (2007) and those obtained by Zhang et al. (2010) using the MSSA for the same experimental data. It was found that none of the soil specimens have the same stress histories and the shapes of the yield curves obtained from the conventional approach are misleading.

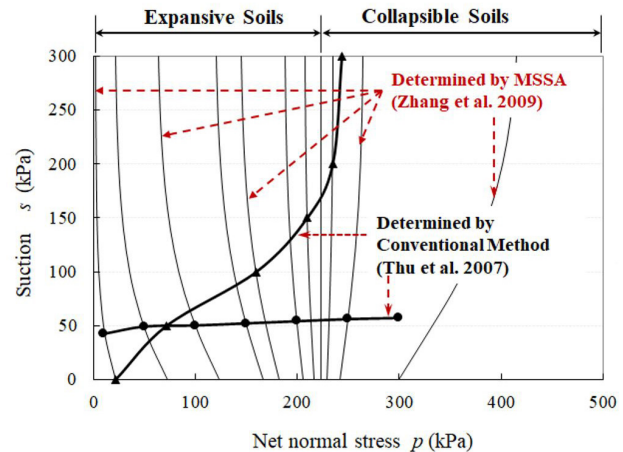


**Figure 4.** Comparison between yield curves obtained from different methods (modified from Zhang et al., 2010).

At present, multiple yield curves are increasingly used to model complicated unsaturated soil behavior, especially when mechanical and hydraulic hysteresis are involved. According to the above discussions, this approach is equivalent to assuming multiple plastic hardening surfaces, or different shapes of the virgin compression lines at different suction levels. The shapes of the virgin compression lines represent soil behavior under isotropic compression, and are best obtained by measurement using laboratory tests. For example, in the BBM, expansion of the LC and SI yield curves form two plastic hardening surfaces of FIJG and HIJC, as shown in Figure 3. Surfaces FIJG and HIJC as shown in Figure 3 are the “traces” of the LC and SI yield curves during their expansions. The evolution of the intersection of the LC and SI yield curves is an intersection curve IJ for the two plastic surfaces. It can be seen that the intersection points of the LC and SI yield curves represent a sharp discontinuity in unsaturated soil behavior, which was considered unlikely by Delage & Graham (1996). No available experimental results support the existence of such a sharp discontinuity.

Another example is the model for highly expansive clays proposed by Alonso et al. (1999) where two yield curves SI and SD, are introduced in addition to the LC yield curve, as well as a microstructural NL yield curve, as shown in Figure 5a. Alonso et al. (1999) use this multi-yield curve model to simulate strain accumulation due to plastic volume change resulting from wetting-drying cycles, taking into account the interaction between the macro and micro-structures, as shown in Figure 5a. A schematic plot of the corresponding elastic and elastoplastic surface of the Alonso et al. (1999) model is shown in Figure 5b. More experimental results are needed to prove or disapprove the assumed shapes of these added yield curves. The SI and SD yield curves are frequently used to simulate the hydraulic hysteresis of the degree of saturation during wetting-drying cycles as well as to obtain a good match between the measured and predicted volume change. Little effort, however, has been placed on



predictions is necessary but not sufficient. Instead, the proposed constitutive model must simultaneously predict many constitutive behaviors of the same soil, in a consistent way. For example, as shown in Figure 3 and Figure 5b, the shapes of the various plastic yield surfaces of the BBM and BExM are significantly different from that of the experimental data by the researchers (e.g., Figure 1). The major reason that the plastic yield surfaces of these models deviate from the experimentally-determined virgin loading surface is caused by assumptions made in the introduction of the SI and SD yield curves. The discrepancy in the shape of the virgin loading surface between multi-yield surface models and experimental data can give the impression that elastoplastic models are dealing with unsaturated soil behavior that is significantly different from that observed by early researchers using SSA methods. Of course, this is not the case.

Since unsaturated soil behavior is closely related to the shape of yield curve, better representation of yield curve is needed to simulate the wetting –induced welling at a low confining stress and the wetting-induced collapse at a high confining stress for unsaturated soils in a unified system. Zhang & Lytton (2009b) analyzed the possible shape of yield curve for unsaturated expansive soils. According to the definition, the yield curve is the boundary separating the elastic and elastoplastic zones. Moving along the yield curve is a neutral loading process and will not generate plastic deformation. In an incremental formulation, the yield curves can be expressed as follows,

$$d\varepsilon_v^p = (m_1^s - m_1^{se}) dp + (m_2^s - m_2^{se}) ds = 0$$

(On the yield curves) (18)

where  $m_1^s$  = coefficient of total volume change with respect to mechanical stress in the elastoplastic zone,  $m_1^s = [1/(1+e_0)] \partial e / \partial p$ ,  $e_0$  is the initial void ratio,  $m_1^{se}$  = coefficient of volume change with respect to mechanical stress in the elastic zone, or bulk modulus of the soil in the elastic zone,  $m_1^{se} = [1/(1+e_0)] \partial e^e / \partial p$ ,  $m_2^s$  = coefficient of total volume change with respect to changes in the matric suction in the elastoplastic zone,  $m_2^s = [1/(1+e_0)] \partial e / \partial s$ , and  $m_2^{se}$  = coefficient of volume change with respect to changes in matric suction or coefficient of expansion due to matric suction change in the elastic zone  $m_2^{se} = [1/(1+e_0)] \partial e^e / \partial s$ .

Using Equation 18, Zhang & Lytton (2009b) analyzed the signs of the partial derivatives of the state boundary surfaces for the shapes of the BBM LC curve, and the represented unsaturated soil behavior. It was found that in the BBM, both  $m_1^s$  and  $m_1^{se}$  have negative signs on the LC yield curve and  $|m_1^s| > |m_1^{se}|$  as shown in Equations 9 and 12 respectively, representing that soil is compressed by the applied mechanical stress, and can yield due to p-loading

under constant matric suction if the soil stress state is on the yield curve. As represented by Equations 10 and 13, respectively,  $m_2^s$  is positive while  $m_2^{se}$  is negative. For the BBM LC conditions on soil parameters, Equation 16 results in that, on the yield curve, the yield stress will increase with an increase in the matric suction, as suggested by Alonso et al. (1990). A positive  $m_2^s$  is the key for successfully predicting collapsible soil behavior in the BBM because it leads to a reduction in the soil volume (collapse) upon wetting under constant net-normal stress. An LC yield curve with a shape that increases the net-normal stress for increasing suction predicts plastic (irrecoverable) volumetric strain when there is a decrease in matric suction and therefore a positive  $m_2^s$  leads to a reduction in the soil volume upon wetting. This was the reason why surface FIJG in Figure 3 was called “Plastic Collapsible Surface” by Zhang & Lytton (2009a, b).

In contrast, on surface HIJC (Figure 3), as well as the SI yield curve in Figure 3,  $m_2^s$  is negative, and  $m_2^{se}$  is also negative. Such a combination can be used to simulate an irrecoverable decrease in the soil volume with an increase in the matric suction beyond the yield suction and recoverable volume increase upon wetting. This increase in soil volume upon wetting is directly opposite to responses of collapsible soils upon wetting. Swell upon wetting is a typical response for unsaturated expansive soils. Commonly, only highly active clays with significant swelling upon wetting are considered to be expansive soils (Wray, 1995). All unsaturated soils with any plasticity (clay content) can exhibit swell upon wetting under low confinement (and compression upon wetting under high confinement). From the viewpoint of constitutive modeling, the common description of expansive soil as being highly active clays is too limited. All soils that swell upon wetting should be considered to be expansive for modeling purposes. This is why the surface HIJC (Figure 3) is named “plastic expansive surface” in Zhang & Lytton (2009a, b). It was also found that on the BBM plastic expansive surface HIJC, the following relationship exists:

$$m_1^s = m_1^{se} \tag{19}$$

Equation 19 is obtained by comparing Equation 9 and 14, and the condition is a result of the BBM assumption of a horizontal SI yield curve.

On the other hand, in the BExM, Gens & Alonso (1992) and Alonso et al. (1999) introduce two inclined 45° yield lines, SI and SD, to replace the original BBM SI proposal by Alonso et al. (1990), as shown in the  $p$ - $s$  plane of Figure 5a. On the 45° yield lines, both  $m_2^s$  and  $m_2^{se}$  are negative. Through incorporation of the SI and SD curves, the BExM can accommodate suction-change induced plastic expansive soil behavior, required to capture the accumulation of strains under cyclic wetting and drying. However, a 45° yield line means the soil is saturated such that an equal magnitude change in  $p$  or  $s$  yield the same magnitude of

change in volume, and the following equations always hold true on 45° yield lines:

$$m_1^s = m_2^s \text{ and } m_1^{se} = m_2^{se} \quad (20)$$

In the BExM (Alonso et al. 1999), a 45° yield line, NL, is related to the microstructural swelling effect, and two additional functions are proposed to link the micro-structural response to the macro-structural response. It is unlikely that all expansive soils are saturated or have the same shapes of yield curves, in general. In addition, it is challenging to calibrate the additional model parameters in the coupling micro-macro function.

Zhang & Lytton (2009b) argued that it is more reasonable to consider that the BBM and BExM restrictions in Equations 19 and 20 do not exist for unsaturated expansive soils in the general case. Instead, for all soils, saturated or unsaturated, the net total stress increase always results in soil compression and plastic deformation beyond yield stress, which means  $|m_1^s| > |m_1^{se}|$  and both have negative signs. It is not reasonable to assume that Equation 19 is satisfied for saturated or unsaturated soils because the virgin compression line is steeper than then unload line. In addition, Equation 20 does not result in reasonable conclusions for unsaturated soils, in general, because the 45° line of the SI and SD curves can only exist for saturated soil conditions. Further, when the restrictions of Equations 19 and 20 are removed, application of Equation 18 to stress states associated with volume increase upon wetting (expansion), gives yield curves on which suction decreases are associated with an increase in the net total stress as shown in Figures 6a and 6b. For stress states corresponding to volume decrease upon wetting (collapse), Equation 18 will result in yield curves on which suction increases are associated an increase in net total stress, as shown in Figure 3a. Equation 18, without restrictions of Equations 19 and 20, as shown in Zhang & Lytton (2009b), is sufficiently general to accommodate volume change of expansion (Figure 6a), collapse (Figure 3), or both (Figure 4 and 7a).

Advantages of the above flexibility in use of Equation 18 was verified by reanalyzing the experimental results reported by Thu et al. (2007) as was shown in Figure 4. A yield curve on which yield stress decreases with an increase in the suction is very important for the constitutive modeling of unsaturated expansive soil behavior. Many soil behaviors, which were considered very complex previously such as those reported by Brackley (1975) and Justo et al. (1984) (Alonso, 1998), can now be easily modeled. For example, in the original BBM, this is considered illogical and the preconsolidation pressure  $p_0^*$  is restricted to be greater than  $p^c$  (Alonso et al., 1990; Wheeler et al., 2002) because a  $p_0^*$  less than  $p^c$  will lead to a decrease in the preconsolidation stress with an increase in the matric suction on the yield curve. By removing this

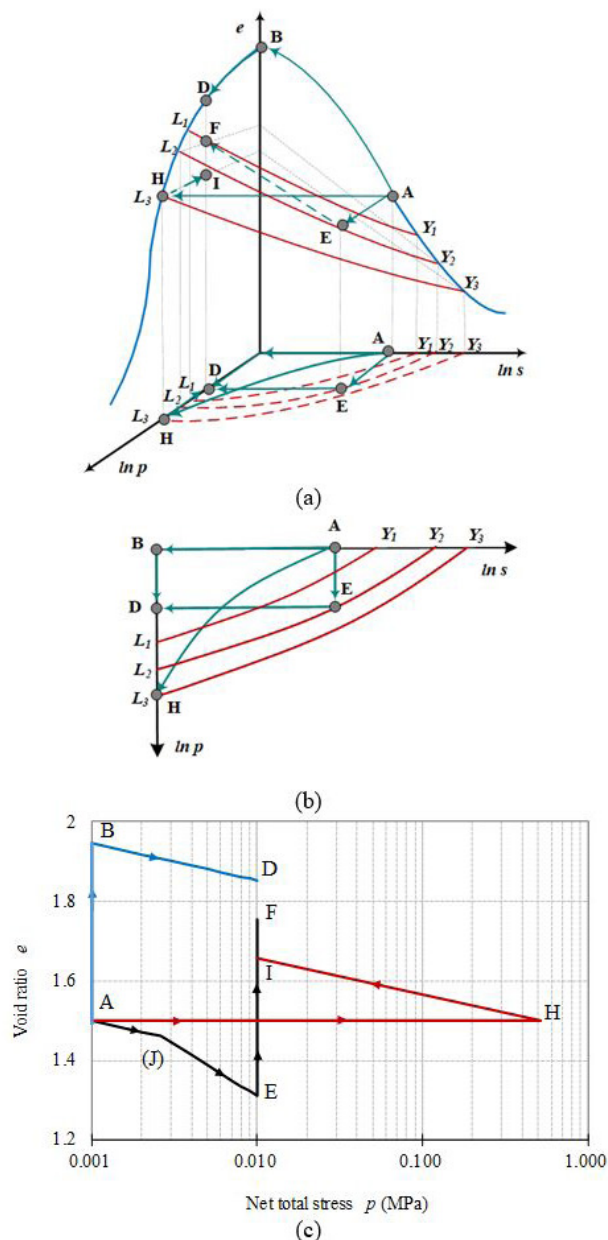


**Figure 6.** Simulation of experimental work by Brackley (1975) for Unsaturated Expansive Soils: (a) schematic plot in the  $e$ - $p$  space; (b) stress paths in the  $p$ - $s$  plane; (c) predicted test results.

restriction ( $p_0^* > p^c$ ) the SI yield curve in the BBM can be discarded while expansive soil behavior can still be simulated.

Figure 6 shows the model predictions of the experimental results by Brackley (1975) using the MSSA, which includes three different tests on compacted high-plasticity clay with complex stress paths as follows: (i) first wetting from A to B and then loading the saturated specimen to a designated stress D ( $A \rightarrow B \rightarrow D$  as shown in Figure 6a), (ii) loading first to the target confining stress and then wetting ( $A \rightarrow E \rightarrow F$  as shown in Figure 6a), and (iii) confining the sample to the swelling pressure and unloading it to the target confining

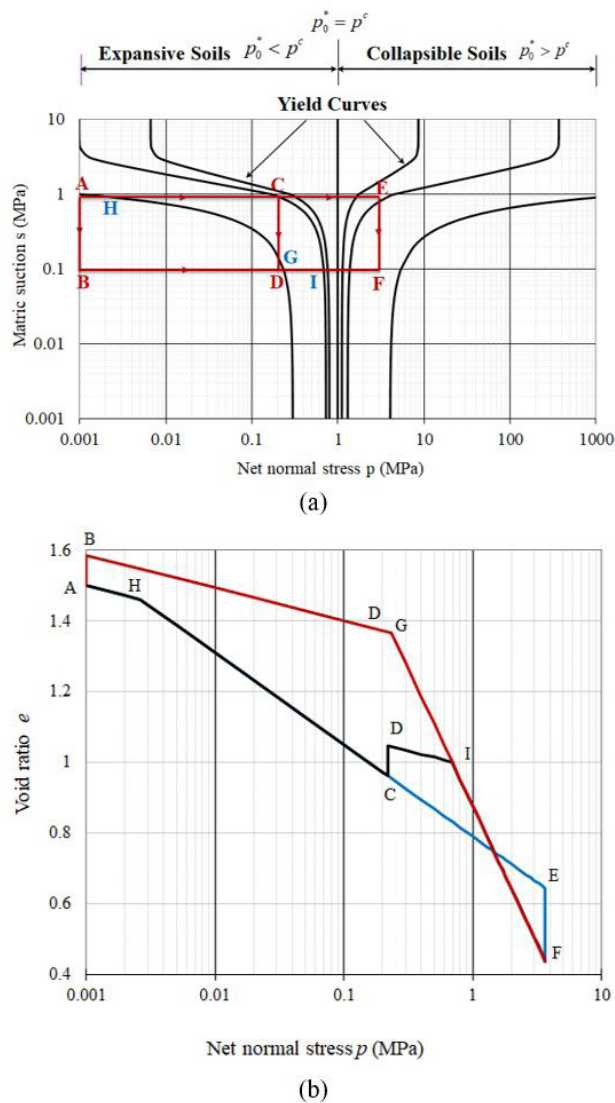


**Figure 7.** Prediction of Both Expansive and Collapsible Behavior in a Unified System: (a) MSSA Simulated Shapes of Yield Curves and Example Stress Paths; (b) predicted unsaturated soil response for stress paths in (a) (modified from Zhang & Lytton, 2009b).

stress (A→E→H→I as shown in Figure 6a). Similar tests were performed by Justo et al. (1984) and are considered as typical unsaturated expansive soil behavior (Alonso, 1998). Figure 6b shows the projection of the yield curves and stress paths in the  $p$ - $s$  plane. The yield curves have shapes of yield stress decreases with an increase in the suction, which is invoked to model unsaturated expansive soils. Figure 6c shows the predicted results, which are qualitatively consistent with the results from Brackley (1975) and Justo et al. (1984).

Zhang & Lytton (2009b) demonstrated that the MSSA can be used to model the behavior of both unsaturated expansive and collapsible soils in a unified system (Figure 7). Figure 7a shows the shapes of the yield curves used by Zhang & Lytton (2009b) to simulate the Brackley (1975) data. When

$p_0^* < p^c$ , unsaturated expansive soil behavior is simulated. When  $p_0^* = p^c$ , the LC curve is a vertical straight line, which is a transition from expansive soil behavior to collapsible soil behavior. When  $p_0^* > p^c$ , unsaturated collapsible soil behavior is simulated. The transition from the expansive soil behavior to collapsible soil behavior is smooth and the corresponding void-ratio constitutive surface has continuous first derivatives with respect to both the net total stress and the matric suction. Figure 7b shows the predicted results for different stress paths. As can be seen in Figure 7b, wetting the soil at a low net total stress of 0.2 MPa results in volume increase (swelling) from point C to D, while wetting the soil at a high net total stress of 3 MPa results volume decrease (collapse) from point E to F. The obtained plastic hardening surface is a warped surface similar to that as shown in Figure 1 on which soil behavior can smoothly change from expansive soil behavior at a low confining stress to collapsible soil behavior at high confining stress level.

In a summary, Figures 4, 6, and 7 show the applications of the MSSA to simulate either collapsible or expansive, or both collapsible and expansive soil behavior in a unified way. In fact, for any warped void ratio surface, such as Equation 17 (Lloret & Alonso, 1985), the MSSA framework can be used to simulate wetting-induced swelling at a low confining stress and wetting-induced collapse at a high confining stress for unsaturated soils, provided a smooth function can be well-fitted to laboratory test results. Under isotropic conditions, it is only required to separate the conventional void ratio surface into an elastic surface (most researchers used Equation 1) and an elastoplastic state boundary surface based upon the MSSA, and to obtain a smooth function for these surfaces. The MSSA, therefore, also represents a smooth bridge across the gap between the traditional state surface approach and elastoplastic constitutive models for unsaturated soils.

One limitation of the original MSSA is that the mechanical and hydraulic hysteresis due to cyclic drying-wetting cycles was not considered. Simulation of such behavior requires incorporating the concept of bounding surface and kinematical hardening, as proposed by Dafalias & Herrmann (1982) and Pastor et al. (1990). This can however be handled with relative simplicity by using the MSSA with an additional new reloading surface which shares the same shapes of yield curve as for the unloading surface. This has been demonstrated in Riad & Zhang (2020, 2021) and is beyond the scope of this paper.

## 4. Oedometer-based models for practice as viewed within an elastoplastic framework

### 4.1 Background

For most practice-based foundation engineering problems it is not necessary to consider the entire state surface for the

soil, or to implement all elements of an elastoplastic model. However, it is always necessary that soil volume change constitutive models, regardless of level of simplification, remain consistent with known unsaturated soil response. It is required, for example, that any volume-change method remains true to the two stress-state unsaturated soil principles. The MSSA was also used to provide a rigorous elastoplastic interpretation of  $K_o$  loading conditions for both saturated and unsaturated soils (Riad & Zhang, 2019; Zhang et al., 2016a, b). Herein, the MSSA is used as an effective framework from which to evaluate simplified  $K_o$  approaches for expansive and collapsible soil volume change analyses used in routine foundation design.

For foundation design, it is often adequate to assume 1-D,  $K_o$  conditions. For this reason, the oedometer device is used extensively in practice for the laboratory testing of expansive and collapsible soils. The ASTM D4546 (ASTM, 2014) response-to-wetting testing is routinely used in the characterization of collapsible and expansive soil sites (Noorany, 2017; Noorany & Houston, 1995; Houston, 2014; Nelson et al., 2006, 2015, Fredlund et al., 2012; Adem & Vanapalli, 2015; Houston, et al., 1988; Washington, 1971). Although several options exist within the ASTM D4546 procedure, Method B is often used in the USA to determine the response of an undisturbed (or representative compacted) specimen of soil to full submergence (full wetting to  $s = 0$ ), starting from field moisture (suction) and field net total stress (vertical stress) conditions (Houston, 2014; Nelson, et al., 2015). Traditional consolidometer testing equipment is used for the ASTM D4546 test, the net total stress (vertical stress) is held constant at the field value of overburden stress, the soil matric suction is reduced to zero by submergence, and no soil suction measurements are made. In performance of the ASTM D4546, Method B, response to wetting test, a field-appropriate soil-wetting path, along a small subset of the entire unsaturated soil state surface, is followed. This type of approach to soil testing and property determination is analogous to the stress path method proposed by Lambe (1967). By testing two or more companion specimens under a range of total stress values, the ASTM D4546, Method B, test can also be used to determine the applied stress level at which the void ratio of the specimen would just remain at its initial value when wetted to  $s = 0$  conditions (i.e., the swell pressure for an expansive soil).

Another commonly used oedometer test for expansive soils is the constant volume test, wherein an undisturbed specimen is placed within the oedometer rings, and vertical load is added to the specimen so as to keep the specimen volume constant during submergence. When, prior to wetting, the specimen is first loaded at in-situ moisture to field overburden, the stress that has to be applied to the specimen to avoid volume change upon submergence is termed the swell pressure, or the constant volume swell pressure,  $\sigma_{OCR}$ . In the USA, the swell pressure is often empirically estimated using a load-back test, wherein the load on the D4546 test

specimen (ASTM, 2014), after full wetting, is increased so as to return the swelled specimen back to its original height (ASTM D4546, Method C, loading-after-wetting test).

Here, some of the available oedometer-based methods for estimation of soil heave and soil collapse under 1-D,  $K_o$ , monotonic wetting conditions are reviewed in the context of elastoplastic volume change models and the unsaturated soil state surface. Currently, most 1-D,  $K_o$ , methods for estimation of volume change of unsaturated soils have been focused on expansive soils, and much less on collapsible soils. Adem & Vanapalli (2015) and Vanapalli & Lu (2012) provide comprehensive reviews of several methods used in the estimation of 1-D volume change of expansive soils, including methods by Briaud et al. (2003), Wray et al. (2005), Lytton (1997), Adem & Vanapalli (2013), Overton et al. (2006), and Vu & Fredlund (2004). Li et al. (2016) provide a general discussion of methods used for estimation of volume change for collapsible soils, although the methods reviewed are not focused on 1-D,  $K_o$ , monotonic wetting conditions. The review here is more limited, and primarily directed at the evaluation of simplified 1-D approaches in the context of more general SSA and elastoplastic methods, via the MSSA. Methods that do not directly, or at least indirectly, consider both soil suction and net total stress as controlling stress state variables are not consistent with known unsaturated soil response and are not considered here. Particular attention will be given to the surrogate path method (SPM), an oedometer-based method that can be used to estimate volume change of expansive or collapsible soils in response to suction change under field net total stress conditions (Singhal, 2010; Houston & Houston, 2018).

#### 4.2 Fredlund method: oedometer based heave analyses

Fredlund & Morgenstern (1976) present the following incremental model for volume change of unsaturated soils in response to isotropically induced changes in suction and net mean total stress:

$$d\varepsilon_v = \frac{de}{1+e_0} = m_1^s dp + m_2^s ds \quad (21)$$

where  $m_1^s$  is the slope of the void ratio-net mean stress plane of the state surface and  $m_2^s$  is the slope of the matric suction plane of the state surface, and  $\varepsilon_v$  = volumetric strain.

Equation 21 was extended to 3-D by Fredlund & Rahardjo (1993), but is not shown here. In principle, Equation 21 is for either expansive or collapsible soils, depending on the sign of  $m_2^s$ , as discussed by Fredlund & Rahardjo (1993). However, considerably more attention was given to use of Equation 21 for soils exhibiting expansion in response to monotonic decrease in suction (wetting). For isotropic loading of an expansive soil, the unsaturated soil volume-change coefficients,  $m_1^s$  and  $m_2^s$ , can be related to the 1-D  $K_o$  loading coefficients,  $C_s$  and  $C_m$  (Figure 8). For 1-D,  $K_o$

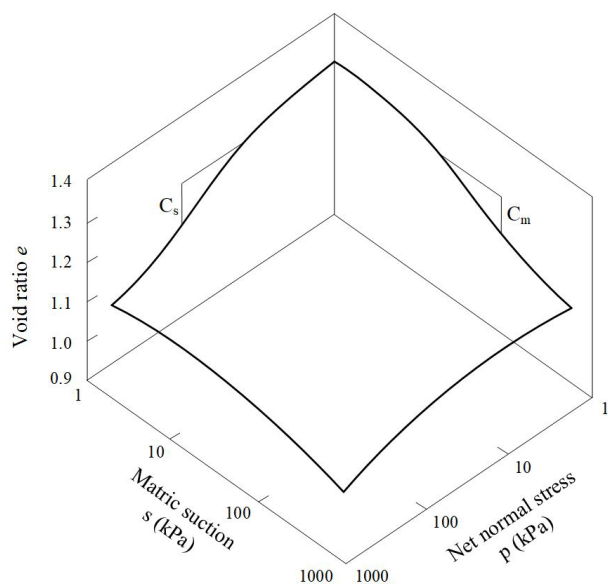


**Figure 8.** State Surface for Expansive Soils (modified from Fredlund & Rahardjo, 1993).

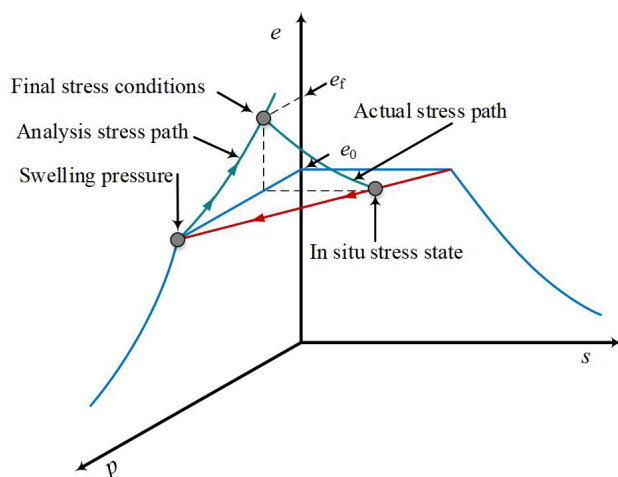


**Figure 9.** Schematic of the Fredlund Method for expansive soil showing an equivalent stress path approach for computation of heave from oedometer tests.

conditions, under an assumption of  $K_0 = 1$ , the volume change coefficients shown in Figure 8 and Equation 21 are related as follows:

$$m_{1-1D}^s = \frac{0.434}{1 + e_0} \frac{C_s}{(\sigma_v - u_a)} \quad (22)$$

$$m_{2-1D}^s = \frac{0.434}{1 + e_0} \frac{C_m}{s} \quad (23)$$

where  $m_{1-1D}^s$  = coefficient of total volume change with respect to mechanical stress under 1-D constrained loading,  $m_{2-1D}^s$  = coefficient of total volume change with respect to

changes in the matric suction under 1D constrained loading,  $C_s = K_0$  loading coefficient corresponding suction,  $C_m = K_0$  loading coefficient corresponding net total stress,  $u_a$  = pore air pressure, and  $\sigma_v$  = net vertical stress.

In the Fredlund oedometer-based 1-D method for estimation of soil heave (Fredlund & Rahardjo, 1993; Fredlund et al., 2012), the concept of an “equivalent matric suction” is used to translate the actual stress path (wetting of the soil in the field under constant net total stress conditions) onto the net total stress plane. The translated (or analysis, or surrogate) stress path in the total stress plane ( $s = 0$  plane), is shown in Figure 9. When suction is plotted on a logarithmic scale and  $s = 0$  is cited herein, it means that  $s$  is so small that there is no significant difference in the void ratio plotted on the lowest depicted suction plane and the void ratio for truly  $s = 0$  conditions. The constant volume oedometer tests is used in the translation (mapping) of the in-situ soil stress state (in terms of net total stress and suction) onto the net total stress plane ( $s = 0$ ). The swell pressure becomes the point on the  $C_s$  sloped curve (in the net total stress plane) where swell strain is zero upon full wetting of the specimen. The constant volume swell pressure, which Fredlund et al. (2012) recommend be corrected for sampling disturbance, is interpreted as the in-situ stress state of the specimen (overburden pressure plus matric suction equivalent). Fredlund & Rahardjo (1993) and Fredlund et al. (2012), place emphasis on measurement of the swell pressure, because the swell pressure is taken to be representative of the initial stress state of the soil. Fredlund et al. (2012) use the swell pressure, together with the matric suction equivalent concept, in lieu of measurement of the initial soil suction.

Once the swell pressure of the expansive soil is determined, Fredlund & Rahardjo (1993) provide numerous methods for obtaining the slope of the translated (analysis) state surface in the total stress plane,  $C_s$  (the swell index), as follows. Upon completion of the constant volume swell test, the specimen (remaining in the consolidometer device) is loaded to a stress well above the swell pressure, and then unloaded (i.e., a saturated soil consolidation test is performed on the constant volume swell test specimen). The slope of the unloading curve, from the post-constant volume swell pressure consolidation test, is defined as  $C_s$  under an assumption of saturated soil conditions and elastic soil state (unload conditions). Fredlund & Rahardjo (1993) also allow use of the unloading curve from a loading-after wetting free swell test as  $C_s$ , as well as determination of  $C_s$  from the unload curve of a traditional consolidation test on saturated soil. Estimation of  $C_s$  from a shrinkage curve (ASTM, 2018) or through correlations with Atterberg limits (Washington, 1971; Lytton, 1994), is also allowed. Fredlund & Rahardjo (1993) assert that problematic heave is commonly attributable to wetting at shallow depth, where net total stress values are relatively low, hence, their allowance for use of the token-load free swell test and token load constant swell pressure, in estimation of the volume-change soil parameters.

Fredlund et al. (2012) provide for the same methods of determination of  $C_s$  as Fredlund & Rahardjo (1993), but also include use of ASTM D4546 (ASTM, 2014) Method A or C (swell tests on “companion” specimens at various surcharge pressures) to obtain  $C_s$ . The use of multiple swell test specimens to define  $C_s$  addresses observed stress path/net total stress level dependencies of response-to-wetting of unsaturated soils (Justo et al., 1984; Noorany & Stanley, 1994; Noorany & Houston, 1995; Houston & Nelson, 2012; Houston et al., 1988).

In the Fredlund Method, the swell pressure and the slope,  $C_s$ , are used to establish the translated (analysis) stress path (Figure 9). Void ratio change in response to reduction of soil suction is estimated as follows:

$$\Delta e = C_s \log \left( \frac{P_f}{P_0} \right) \quad (24)$$

where  $\Delta e$  = change in void ratio between initial and final stress states (i.e.,  $e_f - e_0$ ),  $e_0$  = initial void ratio,  $e_f$  = final void ratio,  $C_s$  = swelling index,  $P_0$  = initial stress state is assumed to be equal to the sample disturbance-corrected swelling pressure, and  $P_f$  = final stress state.

The final stress state,  $P_f$ , includes net total stress changes and suction changes. The final suction conditions must be determined to compute the final stress state,  $P_f$ .

$$P_f = \sigma_v \pm \Delta \sigma_v - u_{wf} \quad (25)$$

where  $\Delta \sigma_v$  = change in total vertical stress due to the excavation, (i.e.,  $-\Delta \sigma_v$ ), or placement of fill (i.e.,  $+\Delta \sigma_v$ ), and  $u_{wf}$  = final pore-water pressure (final matric suction).

Using an incremental-elastic formulation of Equation 21, Vu & Fredlund (2006) provide for highly nonlinear stress state surface curves.  $C_s$  (in Equation 24) can be made to be very small in the low suction or low “translated” net total stress range, avoiding unrealistically large swell strain estimates due to the logarithm relationship assumed between void ratio and suction (and void ratio and net total stress).

In using the final pore-water pressure (suction) directly to define  $P_f$  (Equation 25), there is an underlying assumption that the expansive soil volume change occurs under saturated soil conditions (effective stress principles apply). Fityus & Buzzi (2009) also suggest the treatment of expansive soils as saturated. Vu & Fredlund (2004) introduce the degree of saturation as an empirical operator on the suction to establish the equivalent matric suction value to account for the fact that an equal magnitude change in soil suction and net total stress do not have the same effect on volume change. Fredlund et al. (2012) assert that, for expansive clays, any difference between the actual in-situ matric suction and the “equivalent matric suction” is primarily attributed to the difference in degree of saturation.

Fredlund et al. (2012) interpret the translated stress path line, having slope  $C_s$  in the net total stress plane, as a rebound curve, and therefore an elastic unload-reload surface. This conclusion is reached through the reasoning that field desiccated clay soils possess a very high pre-consolidation stress, such that the swell pressure is always lower than the pre-consolidation stress.

#### 4.3 Use of the MSSA to study test methods used in determination of $C_s$

Elastic (loading/unloading) response-to-wetting response seems to be a reasonable assumption for natural soils subjected seasonally to very wet (near  $s = 0$ ) cyclic conditions. However, for deeper field specimens and compacted specimens not previously subjected to full wetting to  $s = 0$ , the response-to-wetting would seem to be elastoplastic, in general. Therefore, within the framework of the MSSA, the volume change constitutive model of Fredlund & Rahardjo (1993) and Fredlund & Morgenstern (1976) could be considered as a state surface comprised of an elastic (reload/unload) segment and an elastoplastic (virgin loading) segment, depending on the soil stress history. For monotonic loading it is not necessary to separate the elastic and plastic components of volume change. However, it is necessary to consider the elastic and/or plastic nature of specimen response in the interpretation and use of laboratory oedometer tests, because there are implications with regard to the manner in which  $C_s$  is best determined for use with the Fredlund Method. The following discussion uses the MSSA to visualize stress paths commonly used in oedometer-based heave computations.

Figure 10 shows the unsaturated soil state surface corresponding to Figure 9 in  $\ln s$ - $\ln p$  space. In Figure 10, the

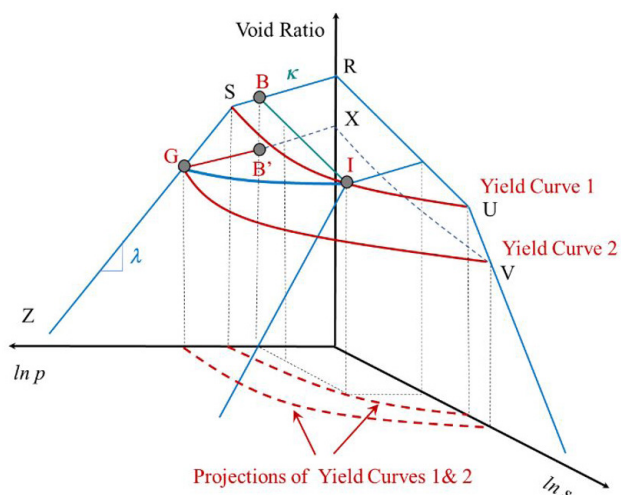


**Figure 10.** Use of the MSSA for interpretation of methods for obtaining  $C_s$ .

state surface is assumed to be elastoplastic (and therefore unique for isotropic loading). For 1-D,  $K_0$  conditions, under an assumption of  $K_0 = 1$ , the volume change coefficients are shown in Figures 8 and 10 are related as follows:

$$m_{1-D}^s = \frac{0.434 C_s}{1 + e_0 (\sigma_v - u_a)} = \frac{1}{1 + e_0} \frac{\lambda(0)}{(\sigma_v - u_a)} \quad (26)$$

$$m_{2-D}^s = \frac{0.434 C_m}{1 + e_0 s} = \frac{1}{1 + e_0} \frac{\lambda_s}{s} \quad (27)$$

Figure 10 shows an example field stress path IB followed under constant in-situ overburden stress and wetting of the soil to  $s = 0$ ; IB is the same as the actual stress path depicted in Figure 9. The path IB is also the path that is followed in the performance of the ASTM D4546 (ASTM, 2014), Method B, oedometer method, assuming that the specimen is essentially “undisturbed” (i.e., returned more or less to its field state upon reloading at in-situ moisture to field overburden stress). At point I, the state of the stress of the soil corresponds to the field suction (in-situ moisture condition) and field total stress (overburden stress). In the sample case depicted in Figure 10, the initial state of stress is assumed to be on a yield curve (i.e., the soil is in a virgin state of stress), and the actual path IB is then an elastic unload process. Figure 10 also shows the stress path of a constant volume wetting test of IG. Because expansive soils exhibit elastoplastic volume-change response, in general, the constant volume swell test can cause the soil to yield, as occurs in the example depicted in Figure 10. The analysis path of Figure 9 corresponds to GB' in Figure 10 for unloading of the soil to field overburden stress at approximately zero suction. Under elastic soil assumptions, in determining the position of B', the slope of GB' is  $\kappa$  (corresponding to  $C_s$ ), determined from an unload consolidation test on a saturated specimen (for example, one performed at the end of a constant volume swell test). Because the constant volume wetting (IG) is a plastic loading process, while the unloading process is elastic, point B' is located on a new elastic surface of GXV, which is below the original elastic surface of RSU. As can be seen, the stress path GB' results in a lower void ratio at field overburden stress compared to the void ratio obtained from the actual field stress path (IB). This result, lower void ratio for path GB' compared to path IB, is confirmed by the laboratory data of Brackley (1975) and qualitative analysis of Zhang & Lytton (2009b) as shown by the stress path A→H→I in Figure 6. Thus, the use of the unloading curve from a saturated specimen consolidation test in the determination of  $C_s$  can result in some degree of underestimate of the field swell strain. Only when paths IB and IG are both elastic are B and B' the same. If, instead,  $C_s$  is determined as the slope GB, where point B is obtained from a D4546, Method B, test, an improved estimate of the

field swell strains is expected because the analysis path would then become GB in the example of Figure 10.

Both the Fredlund Method and the Lytton Method (discussed subsequently) allow for use of the unload curve from a saturated consolidation test for determining  $C_s$ , along with other options. Although Fredlund et al. (2012) provide for the use of the overburden-stress swell test (ASTM D4546, 2014, Method B) to estimate  $C_s$ , Fredlund et al. (2012) does not require a particular oedometer test method of determination of  $C_s$  – rather, Fredlund requires a particular method of determination of swell pressure. Fredlund et al. (2012) argue that the difference between the  $C_s$  value obtained using the overburden swell test (ASTM D4546, Method B) and that obtained from the unloading of a saturated soil specimen (consolidation test) is small. Others, however, point to the importance of path-dependence in the determination of volume change response of unsaturated clays (Noorany & Stanley, 1994; Justo et al., 1984). If the expansive soil is always saturated and the soil volume change is elastic, then the difference between the use of the unload curve from a consolidation test and use of the ASTM D4546, Method B test in establishment of  $C_s$  may be small. If, on the other hand, the soil exhibits an elastic response for field loading conditions, but a plastic response is induced during the constant volume swell test, there may be significant differences in the  $C_s$  values determined by the ASTM D4546 method B test and the  $C_s$  determined from the unloading curve of a consolidation test.

#### 4.4 Nelson method: oedometer based heave analysis

Nelson & Miller (1992) use an approach to estimating 1-D soil expansion that is similar in concept to Fredlund & Rahardjo (1993). The primary difference between the Nelson et al. and the Fredlund & Rahardjo methods relates to the method used to determine the slope of the analysis (translated) state surface in the net total stress plane. Nelson et al. (2015) use the ASTM D4546 (ASTM, 2014), Method B test, performed on an undisturbed (or compacted, representative) specimen of soil under an applied constant stress equal to field overburden, in the determination of full-wetting (to  $s = 0$ ) swell strains. Use of a response-to-wetting oedometer test, performed at in-situ moisture and field overburden stress, in the establishment of fully-wetted field strains is an approach long advocated by Nelson and colleagues for expansive soils (Nelson et al., 1998), as well as by other researchers of both expansive and collapsible soils (Noorany & Stanley, 1994; Noorany & Houston, 1995; Houston et al., 1988; Houston & Nelson, 2012). In the Nelson Method, the ASTM D4546 test, method B, is used together with the swell pressure to obtain  $C_s$ . The advantage of the use of the ASTM D4546, Method B, test for determination of  $C_s$  was previously demonstrated in the example of Figure 10. The slope of the state surface for  $s = 0$  ( $C_s$ , Figure 8) is referred to as the swell index,  $C_H$ , by

Nelson et al. (2006, 2015) when the volume change surface is plotted in terms of vertical strain, rather than void ratio.

The Nelson et al. (2006) approach provides an estimate of the soil volume change (heave) when the soil becomes fully wetted to  $s = 0$  in the field. Based on the research of Chao (2007), Nelson et al. (2015) introduce an empirical approach, based on the degree of saturation, to correct computed swell strains for field wetting conditions resulting in the final degree of saturation less than 100%. In using a degree of saturation-based correction to full-wetting swell strains, the Nelson Method cannot properly account for reduced swell resulting from wetting to final field suction values greater than zero. Except for the special case where field suction is reduced to zero, the Nelson et al. approach to heave computation does not properly consider the effect of both stress state variables, total stress and matric suction. When the final degree of saturation of the field soil is 100%, Nelson et al. (2015) assume that the full-wetting swell strain is achieved, without consideration being given to the actual final field suction value that may exist under full saturation conditions. For expansive clays, the field degree of saturation can be quite high (even 100%) in the presence of rather large suction values due to the relatively high air-entry values of high plasticity clays. Indeed, it is common for an expansive clay heave analysis to proceed under the assumption of saturated soil conditions (Fredlund & Rahardjo, 1993; Fityus & Buzzi, 2009). Provided some significant matric suction remains in the soil after field wetting, the full wetting strain ( $s = 0$  strain, observed in the ASTM, 2014, laboratory test) will not be realized in the field. Thus, the Nelson method, in using degree of saturation, rather than soil suction, to account for partial wetting effects, results in an over-estimate of soil heave in the general case. It is primarily the failure to explicitly consider the role of soil suction, as required when using the MSSA or any other suction-based method, that results in overestimated heave when using Nelson's method.

#### 4.5 The Surrogate Path Method (SPM): oedometer based heave and collapse analyses

##### 4.5.1 Theoretical framework of the SPM

As with the Fredlund and Nelson Methods, the surrogate path method (SPM) considers only a relatively small segment of the 1-D void ratio constitutive surface, obtained under very specific loading conditions: (1)  $K_0$  boundary conditions and 1-D deformation, (2) constant net total stress during wetting, and (3) monotonic decrease of suction (soil wetting) (Singhal, 2010; Houston & Houston, 2018). Although the SPM was originally developed for expansive soils and conditions of soil wetting, the model can also be used to estimate soil collapse and suction increase (drying) shrinkage of expansive soils (Houston & Houston, 2018). For expansive soils, like the Nelson Method, the SPM is anchored to the ASTM D4546 (ASTM, 2014) over-burden swell test results for full

wetting conditions. This ASTM D4546, Method B, test result provides an actual measurement of a point on the  $s = 0$ , net total stress plane of the unsaturated soil state surface. Thus, the SPM is a suction-based method, requiring initial and final soil suction values. As with the Fredlund et al. (2012) method for estimation of soil heave, the SPM requires the estimation of final soil suction values. However, rather than using the constant volume swell pressure and "equivalent matric suction concept" to estimate the initial in-situ soil state, the SPM requires the measurement or estimation of the initial soil suction value. The initial soil suction value can be obtained by different means, including use of relative humidity devices (e.g. WP4C, Meter, Inc.), filter paper, correlations with soil-water characteristic curves, and high capacity tensiometers (Marinho & Teixeira, 2009; Houston & Houston, 2018; Fredlund et al., 2012).

The SPM is based on a two stress-state variable approach to unsaturated soil mechanics, and ensures that the correct (laboratory-observed) soil response is obtained at the endpoints of soil wetting (i.e., at full wetting to final  $s = 0$  and at zero wetting (final  $s =$  initial soil suction value). By using the ASTM D4546 test (ASTM, 2014), performed at overburden stress, the laboratory test specimen is made to follow the same stress path as that of the field prototype, resulting in a direct measurement of soil response for loading to  $s = 0$ . The SPM is a total stress-equivalent or "surrogate" path method, coupled with initial and final soil suction values and oedometer response-to-wetting (submerged specimen) tests (ASTM D4546, 2014).

Figure 11 is a graphical representation of the SPM for an expansive soil. In the SPM, an alternate net total stress path serves as a surrogate path (GQB, Figure 11) to the actual suction-change stress path (IFB, Figure 11a) in reaching the final swell strain,  $\epsilon_B$ , exhibited by an element of soil subjected to full wetting in the field. As with the Fredlund approach, the SPM can be used to estimate an actual segment of the void ratio state surface, such as IFB on Figure 11, for monotonic reduction in soil suction under constant confining stress. However, in practice, preference is for use of the translated (surrogate) stress path along the  $s = 0$  net total stress plane (BQG, Figure 11b). The actual stress path (IFB), corresponding to suction change along a fixed net total stress plane, is not determined directly in the laboratory for the SPM (due to requirements for suction control/measurement devices), but rather full wetting strain AB is estimated using commonly available oedometer tests and testing equipment, without suction control or measurement.

As with the Fredlund Method, the SPM is based on a traditional state surface approach, and it is not absolutely necessary to separate the elastic and plastic strains due to the restriction of the method to monotonic loading (wetting or drying). However, it is of interest to view the SPM within the context of the MSSA to confirm consistency of approach to known elastoplastic unsaturated soil volume-change response, in the general case.

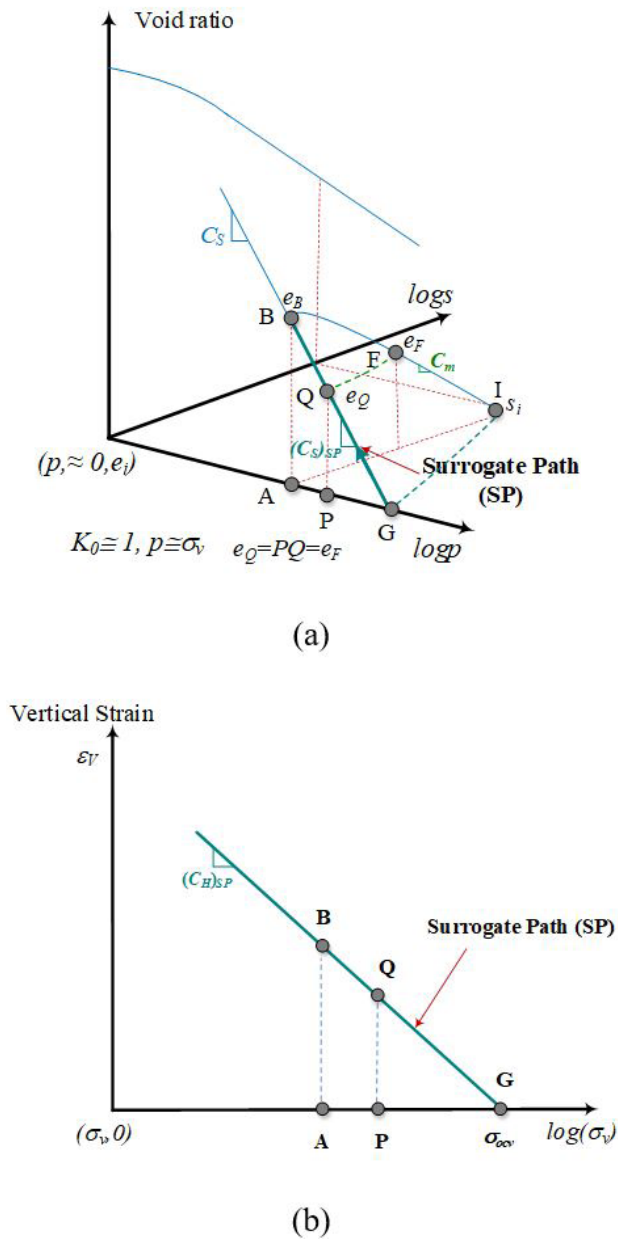


**Figure 11.** Graphical representation of SPM for expansive soils: (a) mapping of actual stress path to net total stress surrogate path; (b) surrogate path used for analysis.

In the SPM, a proportionality factor,  $R_w$  (the ratio of the final suction to the initial matric suction), is used to interpolate ASTM D4546 swell strains (ASTM, 2014) for final suction values intermediate between the initial suction and full wetting (matric suction of zero). As described by Houston & Houston (2018), the actual stress path, with slope  $C_m$ , is the path of line IFB (Figure 11a), where point I is at the original in-situ suction and point F represents the final suction after partial wetting. The void ratio (strain) at point F,  $\varepsilon_F$ , is the desired quantity. The strain for partial wetting,

$\varepsilon_F$ , is obtained by using the proportion of suction dissipated by wetting from I to F as a proportionality factor,  $R_w$ , in estimating the “final” net total stress,  $\sigma_p$ , at point P, Figure 11b.

For the SPM, the ASTM D4546 test specimen (ASTM, 2014) is first loaded at in-situ moisture to field (or prototype) net total stress conditions, and then submerged (fully wetted) under load. For soils that exhibit expansion, the swell index,  $C_H$ , is the slope of the swell strain versus log of “equivalent” total stress, along the “surrogate path” BG, Figure 11b. It is assumed that no swell occurs under constant volume swell pressure,  $\sigma_{ocv}$ , such that the full wetting swell strain,  $\varepsilon_{ob}$ , at overburden stress,  $\sigma_{ob}$  (or overburden plus structural load, as appropriate) is:

$$\varepsilon_{ob} = C_H \log \left( \frac{\sigma_{ocv}}{\sigma_{ob}} \right) \quad (28)$$

where  $C_H$  is the swelling index.

The constant volume swell pressure,  $\sigma_{ocv}$ , can be determined from a constant volume swell test. However, a sufficiently accurate estimate of  $\sigma_{ocv}$  can be obtained by simply performing two swell tests, one at  $\sigma_{ob}$  and one at a substantially higher net total stress and extrapolating to get  $\sigma_{ocv}$  (Houston & Nelson, 2012). Alternatively, the load-back procedure, with correction, can be used to approximate the constant volume swell pressure,  $\sigma_{ocv}$  (Nelson et al., 2006; Olaiz, 2017). The surrogate path BG, is established from the ASTM D4546 test result ( $\varepsilon_{ob}$  at  $\sigma_{ob}$ ) and the constant volume swell pressure, requiring no suction measurements.

The partial wetting strain ( $\varepsilon_{pw}$ ), realized in going from the initial suction value to the final suction value, is:

$$\varepsilon_{pw} = C_H \log \left( \frac{\sigma_{ocv}}{\sigma_p} \right) \quad (29)$$

where

$$\sigma_p = \sigma_{ob} + R_w (\sigma_{ocv} - \sigma_{ob}) \quad (30)$$

$$\text{and } R_w = \frac{s_f}{s_i} \quad (31)$$

where  $s_i$  = initial matric suction and  $s_f$  = final matric suction. The suction proportionality factor  $R_w = 1$  for no wetting and  $R_w = 0$  for full wetting. The strain PQ at point P, along the surrogate path, was compared by Singhal (2010) to the actual strain  $\varepsilon_F$  for numerous cases, and an excellent agreement was found.

Another way to view the SPM is as an interpolation method for going from known (measured) point I to measured point B along the IFB path in Figure 11a. The results of any volume change estimate are constrained to fall between known points I (zero strain) and B (strain at  $s = 0$ ). In establishment of the interpolation method, the ratio of the final to initial soil suction is used, together with an estimate of the constant volume swell pressure. The swell pressure is typically obtained from a load-back swell test (ASTM

D4546, 2014, Method C, loading-after-wetting), or from the log-scale slope of the net total stress path, at  $s = 0$ ,  $C_H$ , established by the full wetting strains of a series of at least two companion specimens at varying applied stress level (ASTM D4546, Method C and Method A). Although direct measurement of the swell pressure might seem ideal, the constant volume swell test is not easy to perform without computer control, and the results are sensitive to any minor swell that occurs during the test, as well as to other system compliances, such as compressibility of the measurement device components (Fredlund et al., 2012). In fact, the constant volume swell test is no longer available as an ASTM Standard. The results for strain obtained by the SPM are not particularly sensitive to the method of estimating the swell pressure (Singhal, 2010; Houston & Houston, 2018). The reason for this is that the SPM requires anchoring of the solution at initial suction ( $R_w = 0$  results in zero volume change) and zero suction (swell strain is that measured by the ASTM D4546 test at  $s = 0$ ). It could be argued that the estimation or measurement of initial suction, using currently available methods, is easier than the measurement of swell pressure. Regardless of one's position on this point, the focus of the SPM on initial and final suction estimation and/or measurement is quite consistent with the two stress-state variable unsaturated soil mechanics principles.

If the ASTM D4546 test specimen (ASTM, 2014) exhibits collapse, the SPM can be used, analogously, for estimation of partial wetting collapse strains (Houston & Houston, 2018). The SPM is used to estimate partial wetting strains,  $\epsilon_{pw}$ , from the D4546 fully wetted collapse strain,  $\epsilon_{ob}$ , by mapping the actual stress path along the void ratio state surface (with slope  $C_m$ ) onto the net total stress plane where  $s = 0$ , and establishing a surrogate path (SP) for collapse (Figure 12).

To establish the slope of the surrogate path, it is necessary to estimate a net total stress,  $\sigma_{G'}$ , for which fully wetted collapse strains are zero. The value of  $\sigma_{G'}$  can be estimated by testing an additional specimen, as identical as possible, using a smaller confining stress equal to 0.2 to  $0.3\sigma_{ob}$ . A straight line on the net total stress plane can be established between the two response-to-wetting test results to establish the surrogate path slope,  $(C_{col})_{sp}$ , analogous to  $(C_H)_{sp}$  for expansive soil. Although it may not be possible to obtain a perfectly identical companion specimen for natural soils, Houston & Houston (2018) report that  $\epsilon_{pw}$  is relatively insensitive to variations in the value of  $\sigma_{G'}$  which can be introduced by sample variability. However, for profiles of high variability in soil cementation, a series of test specimens may be appropriate for establishment of  $C_{col}$  based on an average value of  $\sigma_{G'}$ .

The slope of the surrogate path for collapsible soil,  $(C_{col})$  is:

$$C_{col} = \frac{\epsilon_{ob}}{\log\left(\frac{\sigma_{p'}}{\sigma_{G'}}\right)} \quad (32)$$

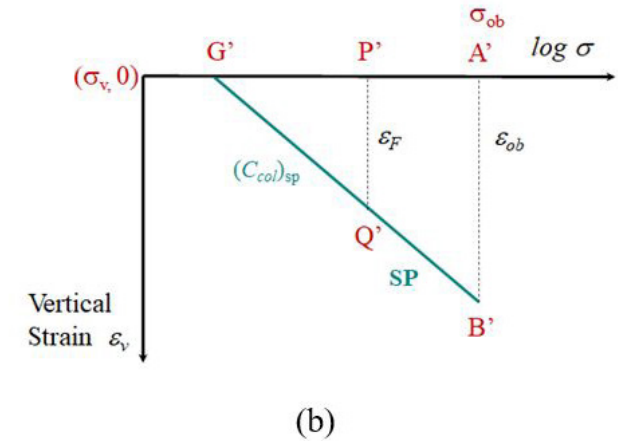
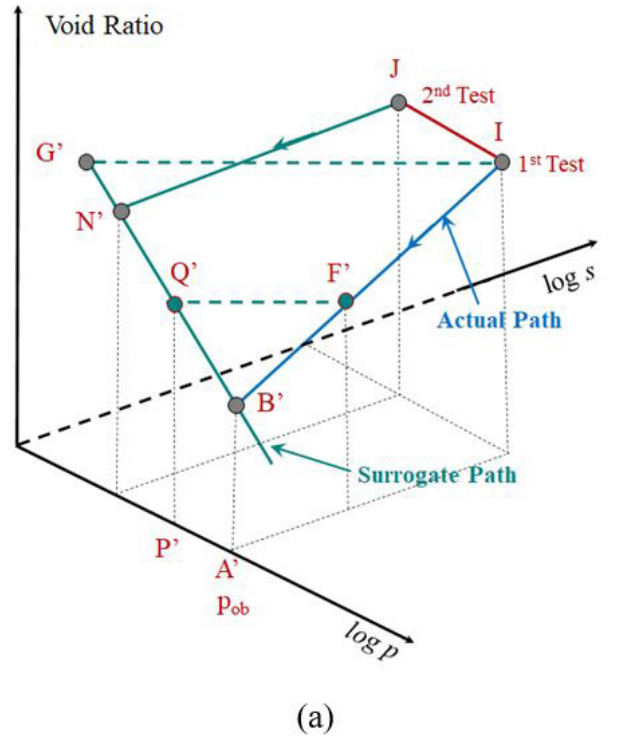


**Figure 12.** Graphical representation of SPM for collapsible soils: (a) mapping of actual stress path to net total stress surrogate path; (b) surrogate path used for analysis.

The partial wetting strain,  $\epsilon_{pw}$ , corresponding to the final suction value for field conditions, is calculated as follows:

$$\epsilon_{pw} = C_{col} \log\left(\frac{\sigma_{p'}}{\sigma_{G'}}\right) \quad (33)$$

$$\text{where } \sigma_{p'} = \sigma_{G'} + (1 - R_w)(\sigma_{ob} - \sigma_{G'}) \quad (34)$$

where  $\sigma_{G'}$  = stress level corresponding to zero volume change upon specimen submergence, and  $\sigma_{p'}$  = surrogate total stress for partial wetting conditions for collapsible soil.

The  $C_{col}$  value for collapsible soil should be given a negative sign to assure that subsequently computed partial wetting collapse strains are compressive. The expression for estimation of partial wetting collapse strains is analogous to that of  $\sigma_p$  for swelling, except that  $(1-R_w)$  is used instead of  $R_w$  because  $\sigma_{ob}$  is greater than  $\sigma_G$ . Due to observed threshold values of suction (degree of saturation) required to induce soil collapse (Houston & Houston, 1997), use of the SPM for collapse is slightly conservative for small degree of wetting of natural cemented soil.

The SPM makes use of oedometer tests performed on relatively undisturbed soil specimens. For natural cemented collapsible soils (not compacted soils), the dry strains observed in loading to appropriate net total stress, prior to wetting, should be added into the fully wetted strain for relatively undisturbed field samples exhibiting collapse, to account for sample disturbance effects (Houston & Houston, 1997). For soils exhibiting expansion upon full wetting, the fully wetted strain should be that associated with re-zeroing the LVDT after first loading “dry” to in-situ stress level, as a means of compensating to some extent for sampling distance. The above corrections for collapsible and expansive soils, respectively, go in the right direction for correcting for sampling disturbance.

#### 4.5.2 Use of the MSSA to evaluate the SPM

The SPM is consistent with the existing elastoplastic framework of unsaturated soils, as can be demonstrated using the MSSA. Figures 13 through 15 demonstrate the application of the SPM, within the context of the MSSA elastoplastic framework, for three example cases (A, B, and C) representing different initial conditions and different volume change responses (expansion or collapse) for unsaturated soil.

For the SPM, the ASTM D4546 test specimen (ASTM, 2014) is first loaded at in-situ moisture to field (or prototype) net total stress conditions, and then submerged (fully wetted) under load. If the net total stress is at a relatively low level, both the wetting path and the surrogate path are expected to fall in the elastic zone as shown for Case A in Figure 13. Point I represents the soil condition at the original in-situ suction and net total stress. The soil is fully wetted along the stress path of IFB, which has the same constant net total stress as that in the field, and point B represents the void ratio at zero suction after full wetting. The surrogate path is QGB, at the zero suction. The instantaneous slope of the surrogate path,  $m_i^s$  ( $C_H$  in log p-log s space), can be obtained by performing an ASTM D4546 test, Method B, to establish point B, and a second ASTM D4546 test, at a different net total stress level, obtaining slope  $C_H$  due to the assumed linear relationship between void ratio and log net mean stress along GQB. Alternatively, where companion specimens are not practical, Point G can be estimated by a load-back test, as described previously – or a constant volume swell test could be performed. For case A, the initial state

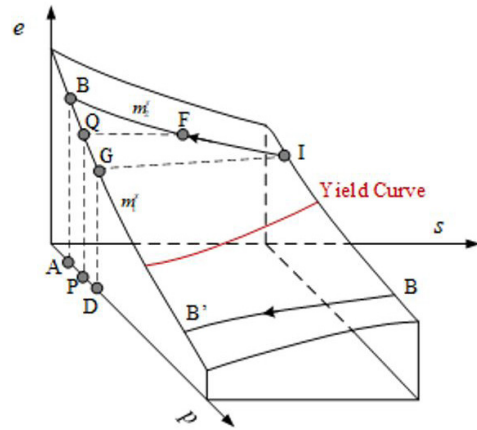


Figure 13. MSSA representation of the SPM under elastic conditions, example Case A.

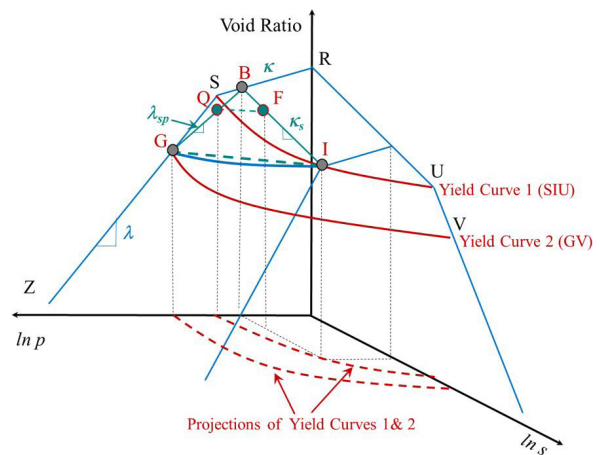


Figure 14. MSSA representation of the SPM for unsaturated expansive soils: example Case B.

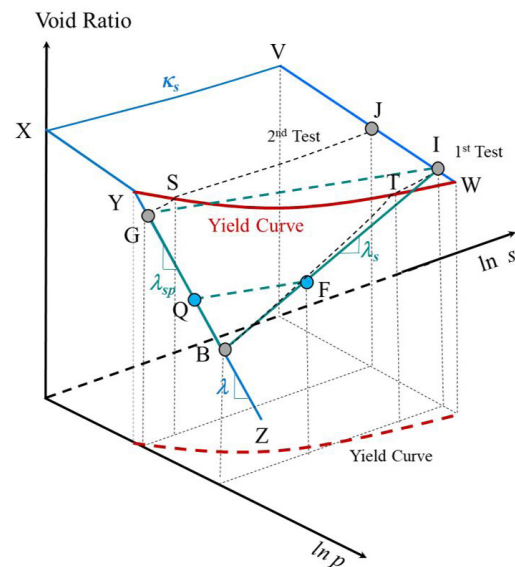


Figure 15. MSSA representation of the SPM for unsaturated collapsible soils: example Case C.

of the soil is in the elastic zone, and the soil remains in the elastic zone during the entire wetting process. As shown in Figure 13, the Case A stress paths, IFB and GQB, are both in the elastic zone. The slope of IFB in Figure 13 is  $m_2^s$  as defined by Fredlund & Rahardjo (1993), corresponding to  $\kappa_s$  in Alonso et al. (1990) where a natural logarithmic scale of suction is used. Using the definitions of Fredlund & Rahardjo (1993), the slope of the surrogate path BQG in Figure 13 is  $(m_1^s)_{sp}$ , corresponding to  $\kappa$  for the natural logarithmic scale of suction used in the Alonso et al. (1990).

In the SPM, if the final soil suction at point F the field is known, then the volume of the soil due to partial wetting can be mapped from point F on the stress path IFB to point Q on the surrogate path GQB using Equations 29, 30, and 31. For case A, where the soil remains in the elastic range during performance of both the ASTM D4546 swell test and for constant volume swell (ASTM, 2014), the SPM gives the correct volume at point Q on the surrogate path. The actual path (IF) follows along the slope  $m_2^s$ , and the surrogate path, QG, follows the correct corresponding state surface (with slope  $m_1^s$ ) in the  $s = 0$  plane.

Figure 14 shows Case B, an example application of the SPM for unsaturated expansive soils wherein the soil remains in the elastic range during the ASTM D4546 swell test (ASTM, 2014), but enters the plastic state during constant volume swell. As shown in Figure 14, surfaces RSU and SGVU represent the elastic and virgin (plastic) state surface of an expansive soil, respectively. The intersection of the elastic and plastic surfaces, SU, represents the initial location of the yield curve. Point I represents the soil conditions at the initial in-situ suction and at the in-situ net total stress, placing the field specimen on the initial yield curve, for Case B. The soil is fully wetted to zero suction along the stress path of IFB under a constant net total stress corresponding to field overburden conditions (ASTM D4546, Method B test). For Case B, this process is fully elastic and the final point B remains in the elastic zone. However, as shown in Figure 14, point G, which has the same void ratio as that of point I, falls on the virgin loading (plastic) surface when the specimen at point I is subjected to a constant volume swell to  $s = 0$ . Point G can be estimated by the load-back method by fully wetting (to  $s = 0$ ) a companion specimen, at net total stress significantly higher than that of point I, to obtain the slope of BQG, assumed linear with slope  $C_{H_s}$ , on the log  $p$ ,  $s = 0$  plane. Of course, point G could also be obtained by running a constant volume swell test. Regardless of the testing method used to obtain point G, yielding of the soil occurs in arriving at point G, and the yield curve expands to the position of the second yield curve, GV, depicted in Figure 14. Regardless of the different possible stress paths followed in arriving at point G, the obtained point G will be the same in that it is on the virgin surface.

When the SPM is used for the situation of Case B, the volume of the soil at partial wetting to point F is obtained by mapping from the stress path IF to point Q on the surrogate

path BQG using Equations 29, 30, and 31. As shown in Figure 14,  $\lambda_{sp}$  (the slope of the surrogate path) is not exactly  $\lambda$  nor  $\kappa$  in the elastoplastic framework. Instead,  $\lambda_{sp}$  represents a mixed effect, given the changes from elastic to elastoplastic zones. However, the SPM still gives the correct volume at point Q on the surrogate path for Case B, because path IFB remains in the elastic range while only the surrogate path crosses from an elastic to a plastic condition. Provided the actual path, IFB, is modeled correctly, the surrogate path does not have to exactly match the actual state surface in the  $s = 0$  plane to obtain the correct void ratio at point Q.

Figure 15 shows Case C, an example application of the SPM for an unsaturated collapsible soil. As shown in Figure 15, surfaces XYWV and YZW represent the elastic and virgin state surfaces, respectively, of a collapsible soil, and YW represents the initial location of the yield curve. Different from the surfaces shown in Figure 14, the state surface for the unsaturated collapsible soil is warped, and the yield stress  $p$  increases with suction along the yield curves, as can be seen by the projection of the yield curve in Figure 15. Point I represents the soil conditions at the original in-situ suction and a relatively high in-situ net total stress, which positions the soil just inside the elastic zone. The soil is fully wetted, under constant field net total stress conditions, along the stress path of IFB to point B at zero suction. This process involves a very small elastic swelling from point I to T, followed by significant wetting-induced collapse caused by plastic yielding of the soil from point T to B.

When the SPM is used for collapsible soil, normally a second wetting test at a stress level lower than that at the field conditions will be performed to obtain the surrogate path GQB. The second specimen has an initial condition of point J, different from the initial condition of point I (in general, the suction level can be different from that of point I as well). The second specimen is wetted under a constant net total stress to point S in the elastic zone, followed by a wetting collapse from point S to G at zero suction. The surrogate path GQB, with slope  $\lambda_{sp}$  is obtained by connecting points G and B.

For known final suction at point F, the SPM can be used to obtain an estimate of the field partial wetting volume change response at point F, corresponding to point Q on the surrogate path. As shown in Figure 15,  $\lambda_{sp}$  is the same as  $\lambda$  in the elastoplastic framework, because points B and G both fall on the virgin surface. When the initial point I is in the elastic zone, as for Case C, IFB is at least somewhat different from the actual stress path of ITB, which can lead to slight overestimate (conservative) estimation of the soil collapse. This overestimate is, however, very small, because the elastic swelling for unsaturated collapsible soil is normally quite small and the soil is typically very close to the yield curve (point W) under normal field conditions. If the collapsible soil is initially on the yield curve, such as having an initial state of point W (Figure 15), then the stress path ITB becomes exactly IFB. Under this situation of an initial state at point W,

the slope of the IFB is the  $\lambda_s$  in the elastoplastic framework, and the estimated partial wetting strain at point Q is correct and not even slightly overestimated.

Cases A, B, and C above demonstrate that the SPM provides good estimates, from the MSSA perspective, of volume change of unsaturated soils under conditions of wetting under constant net stress, whether the soil response is expansion or collapse, and whether the soil has elastic or elastoplastic response, or both. This is a result of the anchoring of the SPM to the correct void ratio response at the endpoints of the surrogate path, points G and B (corresponding, respectively, to the void ratio for no suction change, point I, and the void ratio for suction decrease to  $s = 0$ , point B, along the actual field stress path. Further, the SPM is consistent with, and is easily-visualized within, the elastoplastic framework of the MSSA. As can be seen through the above discussions of cases A, B, and C, point B (Figures 13 to 15) can be guaranteed to fall of the actual  $s = 0$  state surface because the exact field stress path (IFB) is followed in arrival at point B. Point G (or the corresponding G' for the case of collapse), is simply used as a part of the mapping process in going from the actual stress path (IFB) to the  $s = 0$  plane. Therefore, volume change estimates that are adequate for routine engineering foundation design are assured through use of the SPM, provided relatively undisturbed representative specimens are used in performance of the ASTM D4546, Method B test (ASTM, 2014). The soil response modeled using the SPM is consistent with known unsaturated soil volume-change behavior, and the SPM accounts for effects of net total stress in the suction-induced volume change response of unsaturated soil.

#### 4.6 Lytton Method: method of analysis of 1-D heave

The Lytton Method is used extensively in the USA for expansive soil foundation and pavement design purposes. The method has been adopted by the Post-Tensioning Institute (PTI, 2008). The method proposed by Lytton (1977) considers the influence of both net total stress and soil suction in the computation of volumetric strain.

$$\frac{\Delta V}{V_0} = -\gamma_h \log_{10} \left( \frac{h_f}{h_i} \right) - \gamma_\sigma \log_{10} \left( \frac{\sigma_f}{\sigma_i} \right) \quad (35)$$

where  $\gamma_h$  is the slope of the void ratio versus log suction curve when  $p$  is essentially zero, and  $\gamma_\sigma$  is the slope of the void ratio versus log net total stress curve when  $s$  is essentially zero. The net total stress term is only considered until the strains become zero, and soil collapse is not taken into account.

The soil volume change is assumed to be linearly related to the log of soil suction and the log of net total stress. Although Lytton offers oedometer-based methods for determination of the suction index,  $\gamma_h$ , and the compression index,  $\gamma_\sigma$ , emphasis has been placed on empirically-based

approaches to estimation of these suction and compression index values using commonly available soil parameters (PTI, 2008). As with the Fredlund Method, the Lytton approach allows for use of the slope of unload curve from a saturated consolidation test (however, multiplied by 0.7) in determining  $C_s$ , which can lead to underestimates of void ratio where the soil exhibits elastoplastic response during expansion (see Figure 10 and associated discussions). The Lytton Method (PTI, 2008) provides multiple options for estimation of the suction index, and consistency across options cannot be assured, resulting in the potential for differing heave estimates across engineering professionals.

The suction index used by Lytton is conceptualized as the suction index for zero to very light confinement. The effects of suction change and net total stress change are completely decoupled in the Lytton Method. Although the Lytton Method does not directly consider the combined effect of the two unsaturated soil stress state variables, the volume change that occurs in response to change in soil suction is reduced to account for the influence of confining stress (e.g., overburden stress). In the context of the MSSA, because of the decoupling of the suction and net total stress effects, the Lytton Method can be shown to consider only the state surface bounding curves of Figure 8 (i.e., the net total stress plane where  $s$  is essentially zero and the suction plane where  $p$  is essentially zero). Solutions based on the Lytton Method (PTI, 2008) would, in general, be expected to deviate from the MSSA because the path dependency of expansive soil volume change response is not directly addressed, and because the actual field stress path is not required to be followed in the determination of the suction index and the compression index. However, the Lytton Method (PTI, 2008) provides for use of empirically-based (field-calibrated) approaches in the determination of the suction index and compression index, which when used appropriately represent one way to mitigate (reduce) errors in void ratio estimate when using the PTI-based analyses.

## 5. Conclusions

The traditional state surface approach emerged from the recognition that unsaturated soil volume change response is complex and requires the simultaneous consideration of two stress state variables, net total stress and matric suction. One major advantage of the SSA is that the soil model is based upon observed (measured) laboratory unsaturated soil response. If a soil exhibits either expansion or collapse, or both, upon wetting under the range of total net stress conditions of interest, the surface can simply be modified to accommodate. A disadvantage of the traditional state surface approach is that there is no direct way to separate elastic soil response from elastoplastic soil response. This disadvantage becomes more severe when the tested soil specimens do not have the same stress history. In principle, incremental elastic formulations of the state surface, such as that detailed by

Fredlund & Rahardjo (1993), can handle some aspects of elastoplastic behavior, such as accommodating unload/reload via change of elastic modulus. However, the traditional state surface still suffers some difficulties in proportioning elastic and plastic soil components of volume change. Elastoplastic models, starting with the BBM (Alonso et al., 1990), emerged to address some of the challenges posed in using the SSA for unsaturated soils that are known to exhibit elastoplastic behavior. However, in the development of elastoplastic models for unsaturated soils, some of the valuable aspects of the SSA were lost. In particular, as revealed through consideration of the MSSA, the addition of multiple yield surfaces to accommodate elastoplastic expansion and collapse within the same model can result in a void ratio state surface that is inconsistent with available laboratory data when it is viewed in whole. The primary modification that can lead to simplification of most elastoplastic unsaturated soil models is the introduction of greater flexibility in defining the yield surface (i.e. the virgin state surface). Added flexibility in the establishment of the yield curve avoids the need for the introduction of multiple yield surfaces and reduces the number of required soil parameters, in general.

By adopting the relatively simple elastoplastic framework of the MSSA, practice-based oedometer methods can be evaluated for consistency with known unsaturated soil volume change response. In this way, better approaches for estimating volume change consistent with measured field stress-path dependent response can be identified. Further, because of the heavy use of oedometer testing methods for expansive and collapsible soils, it is helpful to explain common test procedures within the unsaturated soil elastoplastic framework. The MSSA was used to demonstrate, through consideration of general elastoplastic soil behavior, the importance of anchoring practice-based solutions to problems of collapse or expansion to field stress-path appropriate laboratory tests. For 1-D,  $K_0$ , constant net total stress field conditions under a path of soil wetting, the ASTM D4546 (ASTM, 2014), Method B, swell test provides the most important anchor point for volume change computation. Another important anchor point is the no-wetting (no suction change) soil response, wherein the soil specimen remains at the initial in-situ void ratio. The SPM (Houston & Houston, 2018) is an oedometer test/suction-based method, requiring: (1) initial and final soil suction values, (2) ASTM D4546, Method B, test results, and (3) a measurement or estimate of the net total stress level that, when applied to the soil specimen, results in zero volume change when suction is brought to zero. The SPM uses a suction value-based mapping to estimate volume change when field wetting is intermediate between no wetting and full wetting corresponding to the ASTM D4546 test. The SPM is based on a two-stress state variable approach to unsaturated soil mechanics, is consistent with known elastoplastic unsaturated soil volume change response, and applies to both expansive and collapsible soils. Major advantages of the SPM include simplicity and bounding of

the problem solution for consistency with path-appropriate measured soil response, which results in consistency of volume change estimates across different users of the method.

Appropriate constitutive models for volume change of unsaturated soil, whether for advanced research or practice-based foundation design, require consistency with observed soil behavior across a full spectrum of stress path conditions. The MSSA is a relatively simple elastoplastic framework that is useful in the evaluation of unsaturated soil volume change constitutive models. The MSSA makes use of the traditional state surface approach (SSA), which was based on laboratory-observed unsaturated soil behavior, requiring the use of two independent stress state variables, net total stress, and suction. Retention of these important features of the SSA in the development of unsaturated soil constitutive models is required to ensure consistency of approaches that geotechnical engineers use, regardless of level of sophistication of model required for the problem at hand.

## Acknowledgements

The authors would like to acknowledge Professor William N. Houston for his valuable review and discussions on this paper, and for his contributions and insight relative to the SPM method. The authors also acknowledge the contributions of graduate students Beshoy Riad and Javad Galinmoghdam for assistance with preparation of figures and formatting of the final manuscript.

## Declaration of interest

The authors have not conflict of interests regarding the material included in this paper.

## Authors' contributions

Sandra L. Houston: writing, reviewing, editing, investigation, methodology. Xiong Zhang: writing, reviewing, editing, investigation, methodology.

## List of symbols

$C_1, C_2, C_3,$ and $C_4$	constants
$a, b, c,$ and $d$	constants
$C_s K_0$	loading coefficient corresponding suction;
$C_m K_0$	loading coefficient corresponding net total stress;
$C_H$	swelling index;
$C_{col}$	collapsing index;
$(C_{col})_{sp}$	collapsing index for surrogate path;
$(C_H)_{sp}$	swelling index for surrogate path;
$m_{1-1D}^s$	coefficient of total volume change with respect to mechanical stress under 1D constrained loading;

$m_{2-1D}^s$	coefficient of total volume change with respect to changes in the matric suction under 1D constrained loading;	$\kappa$	slope of the unloading-reloading line associated with the mean net stress;
$e$	voids ratio;	$\kappa_s$	slope of the unloading-reloading line associated with soil suction;
$e_0$	initial voids ratio;	$\lambda_s$	slope of the virgin compression line associated with soil suction;
$e_f$	final voids ratio;	$\lambda(s)$	slope of the virgin compression line associated with the mean net stress for $s \neq 0$ ;
$\Delta e$	change in void ratio between the initial and final stress states ( $= e_f - e_0$ );	$\lambda(0)$	slope of the virgin compression line associated with the mean net stress for $s = 0$ ;
$R_w$	ratio of the final suction to the initial matric suction values;	$\lambda_{sp}$	slope of surrogate path;
$\Delta V$	volume change;	$m_1^{se}$	coefficient of volume change with respect to mechanical stress in the elastic zone, or bulk modulus of the soil in the elastic zone;
$V_0$	initial volume;	$m_2^{se}$	coefficient of volume change with respect to changes in matric suction or coefficient of expansion due to matric suction change;
$h_i$	initial sample height;	$m_1^s$	coefficient of total volume change with respect to mechanical stress in the elastoplastic zone;
$h_f$	final sample height;	$(m_1^s)_{sp}$	coefficient of total volume change with respect to mechanical stress in the elastoplastic zone for surrogate path;
$K_0$	at-rest earth pressure coefficient;	$m_2^s$	coefficient of total volume change with respect to changes in the matric suction.
$k$	parameter that relates cohesion and suction;		
$M$	slope of theoretical critical state line;		
$N(s)$	specific volume for $p p^C$ ;		
$p$	net mean stress ( $\sigma_m - u_a$ );		
$p_{at}$	atmospheric pressure;		
$p^C$	reference stress;		
$\sigma_v$	net vertical stress;		
$\sigma_{ob}$	overburden stress;		
$\sigma_{ocv}$	constant volume swell pressure;		
$\sigma_i$	initial net stress;		
$\sigma_f$	final net stress;		
$p_0$	apparent preconsolidation pressure at a certain suction;		
$p_0^*$	preconsolidation pressure in saturated conditions;		
$P_0$	initial stress state;		
$P_f$	final stress state;		
$q$	deviatoric stress ( $\sigma_1 - \sigma_2$ );		
$r$	parameter controlling the slope of the virgin compression line;		
$s$	soil suction ( $u_a - u_w$ );		
$s_0$	maximum historical suction applied to the soil;		
$s_i$	initial suction value;		
$s_f$	final suction value;		
$u_a$	air pressure;		
$u_w$	water pressure;		
$u_{wf}$	final pre-water pressure;		
$v$	specific volume;		
$\gamma_h$	slope of the void ratio versus log suction curve when $p$ zero;		
$\gamma_\sigma$	slope of the void ratio versus log net total stress curve when $s$ zero;		
$\beta$	parameter that controls the slope of the virgin compression line for $s \neq 0$ ;		
$\varepsilon_v$	volumetric strain;		
$d\varepsilon_v$	volumetric strain increment;		
$\varepsilon_{ob}$	full wetting swell strain;		
$\varepsilon_{pw}$	partial wetting strain;		
$\varepsilon_v^e$	elastic volumetric strains;		
$\varepsilon_v^p$	plastic volumetric strain;		

## References

- Adem, H.H., & Vanapalli, S.K. (2013). Constitutive modeling approach for estimating 1-D heave with respect to time for expansive soils. *International Journal of Geotechnical Engineering*, 7(2), 199-204. <http://dx.doi.org/10.1179/1938636213Z.00000000024>.
- Adem, H.H., & Vanapalli, S.K. (2015). Review of methods for predicting in situ volume change movement of expansive soil over time. *Journal of Rock Mechanics and Geotechnical Engineering*, 7(1), 73-86. <http://dx.doi.org/10.1016/j.jrmge.2014.11.002>.
- Alonso, E.E, Gens, A., & Gehling, W.Y.Y. (1994). Elastoplastic model for unsaturated expansive soils. In *Proceedings of the 3rd European Conference on Numerical Models in Geotechnical Engineering* (pp. 11-18), Rotterdam.
- Alonso, E.E. (1987). Special problem soils: general report. In *Proceedings of the 9th European Conference on Soil Mechanics and Foundation Engineering* (Vol. 3, pp. 1087-1146). Dublin: CRC Press.
- Alonso, E.E., Gens, A., & Josa, A. (1990). A constitutive model for partially saturated soils. *Geotechnique*, 40(3), 405-430. <http://dx.doi.org/10.1680/geot.1990.40.3.405>.
- Alonso, E.E., Vaunat, J., & Gens, A. (1999). Modelling the mechanical behaviour of expansive clays. *Engineering Geology*, 54(1-2), 173-183. [http://dx.doi.org/10.1016/S0013-7952\(99\)00079-4](http://dx.doi.org/10.1016/S0013-7952(99)00079-4).
- Alonso, E.E. (August 27-30, 1998). Modelling expansive soil behaviour. In *Proceedings of the 2nd International*

- Conference on Unsaturated Soils* (Vol. 2. pp. 37–70). Beijing: International Academic Publishers.
- ASTM D4546. (2014). *Standard test methods for one-dimensional swell or collapse of soils*. ASTM International, West Conshohocken, PA. <https://doi.org/10.1520/D4546-14E01>.
- ASTM D4943. (2018). *Standard test method for shrinkage factors of cohesive soils by the water submersion method*. ASTM International, West Conshohocken, PA. <https://doi.org/10.1520/D4943-18>.
- Barden, L., McGown, A., & Collins, K. (1973). The collapse mechanism in partly saturated soil. *Engineering Geology*, 7(1), 49-60. [http://dx.doi.org/10.1016/0013-7952\(73\)90006-9](http://dx.doi.org/10.1016/0013-7952(73)90006-9).
- Bellil, S., Abbeche, K., & Bahloul, O. (2018). Treatment of a collapsible soil using a bentonite-cement mixture. *Studia Geotechnica et Mechanica*, 40(4), 233-243. <http://dx.doi.org/10.2478/sgem-2018-0042>.
- Blatz, J.A., & Graham, J. (2003). Elastic-plastic modelling of unsaturated soil using results from a new triaxial test with controlled suction. *Geotechnique*, 53(1), 113-122. <http://dx.doi.org/10.1680/geot.2003.53.1.113>.
- Bolzon, G., Schrefler, B.A., & Zienkiewicz, O.C. (1996). Elastoplastic soil constitutive laws generalized to partially saturated states. *Geotechnique*, 46(2), 279-289. <http://dx.doi.org/10.1680/geot.1996.46.2.279>.
- Brackley, I.J.A. (1973). *Swell pressure and free swell in compacted clay*. Pretoria, South Africa: National Building Research Institute, Council for Scientific and Industrial Research.
- Brackley, I.J.A. (1975). Swell under load. In *Proceedings of the 6th Regional Conference for Africa Soil Mechanics and Foundation Engineering* (Vol. 1, pp. 65-70). Durban: National Building Research Institute/CSIR.
- Briaud, J.L., Zhang, X., & Moon, S. (2003). Shrink test-water content method for shrink and swell predictions. *Journal of Geotechnical and Geoenvironmental Engineering*, 129(7), 590-600. [http://dx.doi.org/10.1061/\(ASCE\)1090-0241\(2003\)129:7\(590\)](http://dx.doi.org/10.1061/(ASCE)1090-0241(2003)129:7(590)).
- Casagrande, A. (1936). The determination of preconsolidation load and its practical significance. In *Proceedings of the 1st International Conference on Soil Mechanics and Foundation Engineering* (Vol. 3, pp. 60-64). Cambridge, MA: Graduate School of Engineering, Harvard University.
- Chao, K.C. (2007). *Design principles for foundations on expansive soils* [Doctoral dissertation, Colorado State University Fort Collins]. Colorado State University Fort Collins' repository.
- Costa, L.M., & Alonso, E.E. (2009). Predicting the behavior of an earth and rockfill dam under construction. *Journal of Geotechnical and Geoenvironmental Engineering*, 135(7), 851-862. [http://dx.doi.org/10.1061/\(ASCE\)GT.1943-5606.0000058](http://dx.doi.org/10.1061/(ASCE)GT.1943-5606.0000058).
- Cui, Y.J., & Delage, P. (1996). Yielding and plastic behaviour of an unsaturated compacted silt. *Geotechnique*, 46(2), 291-311. <http://dx.doi.org/10.1680/geot.1996.46.2.291>.
- D'Onza, F., Wheeler, S.J., Gallipoli, D., Barrera Bucio, M., Hofmann, M., Lloret-Cabot, M., Lloret Moranco, A., Mancuso, C., Pereira, J.-M., Romero Morales, E., Sánchez, M., Sołowski, W., Tarantino, A., Toll, D.G., & Vassallo, R. (2015). Benchmarking selection of parameter values for the Barcelona basic model. *Engineering Geology*, 196, 99-118. <http://dx.doi.org/10.1016/j.enggeo.2015.06.022>.
- Dafalias, Y.F., & Herrmann, L.R. (1982). Bounding surface formulation of soil plasticity. In G.N. Pande & O.C. Zienkiewicz (Eds.), *Soil mechanics: transient and cyclic loads* (pp. 253-282). New York: John Wiley & Sons.
- Dangla, P., Malinsky, L., & Coussy, O. (1997). Plasticity and imbibition-drainage curves for unsaturated soils: a unified approach. In *Proceedings of the Numerical Models in Geomechanics: NUMOG VI* (pp. 141-146). Montreal: CRC Press.
- Delage, P., & Graham, J. (1996). Mechanical behaviour of unsaturated soils: understanding the behaviour of unsaturated soils requires reliable conceptual models. In *Proceedings of the 1st International Conference on Unsaturated Soils (UNSAT)* (Vol. 3, pp. 1223-1256). Paris: Balkema.
- Dessouky, S., Oh, J.H., Yang, M., Ilias, M., Lee, S.I., & Jao, M. (2012). *Pavement repair strategies for selected distresses in FM roadways*. Texas: Texas Transportation Institute.
- Dif, A.E., & Bluemel, W.F. (1991). Expansive soils under cyclic drying and wetting. *Geotechnical Testing Journal*, 14(1), 96-102. <http://dx.doi.org/10.1520/GTJ10196J>.
- Driscoll, R.M.C., & Crilly, M.S. (2000). *Subsidence damage to domestic buildings: lessons learned and questions remaining*. Watford, UK: Foundation for the Built Environment (FBE).
- Fityus, S., & Buzzi, O. (2009). The place of expansive clays in the framework of unsaturated soil mechanics. *Applied Clay Science*, 43(2), 150-155. <http://dx.doi.org/10.1016/j.clay.2008.08.005>.
- Fonte, N.L., de Carvalho, D., & Kassouf, R. (2017). Improvement of collapsible soil conditions for industrial floors. In *Proceedings of the International Congress and Exhibition "Sustainable Civil Infrastructures: Innovative Infrastructure Geotechnology"* (pp. 177-193). Switzerland: Springer. [https://doi.org/10.1007/978-3-319-61902-6\\_15](https://doi.org/10.1007/978-3-319-61902-6_15).
- Fredlund, D.G. (1979). Second Canadian Geotechnical Colloquium: appropriate concepts and technology for unsaturated soils. *Canadian Geotechnical Journal*, 16(1), 121-139. <http://dx.doi.org/10.1139/t79-011>.
- Fredlund, D.G., & Morgenstern, N.R. (1976). Constitutive relations for volume change in unsaturated soils. *Canadian Geotechnical Journal*, 13(3), 261-276. <http://dx.doi.org/10.1139/t76-029>.
- Fredlund, D.G., & Morgenstern, N.R. (1977). Stress state variables for unsaturated soils. *Journal of Geotechnical and Geoenvironmental Engineering*, 103(5). <http://dx.doi.org/10.1061/ajgeb6.0000423>.

- Fredlund, D.G., & Rahardjo, H. (1993). *Soil mechanics for unsaturated soils*. New York: John Wiley & Sons. <http://dx.doi.org/10.1002/9780470172759>.
- Fredlund, D.G., Hasan, J.U., & Filson, H. (1980). The prediction of total heave. In *Proceedings of the 4th International Conference on Expansive Soils* (pp. 1-11). Denver: ASCE.
- Fredlund, D.G., Rahardjo, H., & Fredlund, M.D. (2012). *Unsaturated soil mechanics in engineering practice*. Hoboken: John Wiley & Sons. <http://dx.doi.org/10.1002/9781118280492>.
- Gallipoli, D., Gens, A., Sharma, R., & Vaunat, J. (2003a). An elastoplastic model for unsaturated soil incorporating the effects of suction and degree of saturation on mechanical behaviour. *Geotechnique*, 53(1), 123-136. <http://dx.doi.org/10.1680/geot.2003.53.1.123>.
- Gallipoli, D., Wheeler, S.J., & Karstunen, M. (2003b). Modelling the variation of degree of saturation in a deformable unsaturated soil. *Geotechnique*, 53(1), 105-112. <http://dx.doi.org/10.1680/geot.2003.53.1.105>.
- Geiser, F., Laloui, L., & Vulliet, L. (2000). Modelling the behaviour of unsaturated silt. In A. Tarantino & C. Mancuso (Eds.), *Experimental evidence and theoretical approaches in unsaturated soils* (pp. 155-175). London: CRC Press. <https://doi.org/10.1201/9781482283761-15>.
- Gens, A., & Alonso, E.E. (1992). A framework for the behaviour of unsaturated expansive clays. *Canadian Geotechnical Journal*, 29(6), 1013-1032. <http://dx.doi.org/10.1139/t92-120>.
- Gens, A., & Olivella, S. (2001). THM phenomena in saturated and unsaturated porous media: fundamentals and formulation. *Revue Française de Génie Civil*, 5(6), 693-717. <http://dx.doi.org/10.1080/12795119.2001.9692323>.
- Gens, A., Alonso, E.E., & Delage, A. (1996). Constitutive modelling: application to compacted soils. In *Proceedings of the 1st International Conference on Unsaturated Soils (UNSAT)* (Vol. 3, pp. 1179-1200). Paris: Balkema.
- Houston, S.L. (2014). Characterization of unsaturated soils: the importance of response to wetting. In *Proceedings of the Geo-Congress 2014 Keynote Lectures* (pp. 77-96). Atlanta: ASCE. <https://doi.org/10.1061/9780784413289.004>.
- Houston, S.L. (2019). It is time to use unsaturated soil mechanics in routine geotechnical engineering practice. *Journal of Geotechnical and Geoenvironmental Engineering*, 145(5), 2519001. [http://dx.doi.org/10.1061/\(ASCE\)GT.1943-5606.0002044](http://dx.doi.org/10.1061/(ASCE)GT.1943-5606.0002044).
- Houston, S.L., & Houston, W.N. (1997). Collapsible soils engineering. In D. G. Fredlund & S. L. Houston (Eds.), *Unsaturated soil engineering practice geotechnical* (Special Publication, No. 68, pp. 199-232). New York: ASCE.
- Houston, S.L., & Houston, W.N. (2018). Suction-oedometer method for computation of heave and remaining heave. In *Proceedings of the 2nd Pan-American Conference on Unsaturated Soils* (pp. 93-116). Dallas: ASCE. <http://dx.doi.org/10.1061/9780784481677.005>.
- Houston, S.L., Houston, W.N., & Spadola, D.J. (1988). Prediction of field collapse of soils due to wetting. *Journal of Geotechnical Engineering*, 114(1), 40-58. [http://dx.doi.org/10.1061/\(ASCE\)0733-9410\(1988\)114:1\(40\)](http://dx.doi.org/10.1061/(ASCE)0733-9410(1988)114:1(40)).
- Houston, W.N., & Nelson, J.D. (2012). The state of the practice in foundation engineering on expansive and collapsible soils. In *Proceedings of the Geo-Congress 2014 Keynote Lectures* (pp. 608-642). Oakland: ASCE. <https://doi.org/10.1061/9780784412138.0023>.
- Jennings, J.E.B., & Burland, J.B. (1962). Limitations to the use of effective stresses in partly saturated soils. *Geotechnique*, 12(2), 125-144. <http://dx.doi.org/10.1680/geot.1962.12.2.125>.
- Jennings, J.E.B., & Knight, K. (1957). The additional settlement of foundations due to collapse of sandy soils on wetting. In *Proceedings of the 4th international conference on soil mechanics and foundation engineering* (pp. 316-319). London.
- Jones, L. (2018). Expansive soils. In P. Bobrowsky & B. Marker (Eds.), *Encyclopedia of engineering geology* (Encyclopedia of Earth Sciences Series). Cham: Springer. [http://dx.doi.org/10.1007/978-3-319-73568-9\\_118](http://dx.doi.org/10.1007/978-3-319-73568-9_118).
- Jones, L.D., & Jefferson, I. (2012). Expansive soils. In J. Burland, T. Chapman, H. Skinner & M. Brown (Eds.), *ICE manual of geotechnical engineering: geotechnical engineering principles, problematic soils and site investigation* (Vol. 1, pp. 413-441). London: ICE Publishing. <https://doi.org/10.1680/moge.57074>.
- Justo, J.L., Delgado, A., & Ruiz, J. (1984). The influence of stress-path in the collapse-swelling of soils at the laboratory. In *Proceedings of the 5th International Conference on Expansive Soils* (pp. 67-71). Adelaide: Institution of Engineers.
- Khalili, N., & Loret, B. (2001). An elastoplastic model for non-isothermal analysis of flow and deformation in unsaturated porous media: formulation. *International Journal of Solids and Structures*, 38(46-47), 8305-8330. [http://dx.doi.org/10.1016/S0020-7683\(01\)00081-6](http://dx.doi.org/10.1016/S0020-7683(01)00081-6).
- Knodel, P.C. (1992). *Characteristics and problems of collapsible soils*. Denver, CO: US Department of the Interior, Bureau of Reclamation, Research and Laboratory Services Division, Materials Engineering Branch.
- Karube, D. (1986). New concept of effective stress in unsaturated soil and its proving tests. In *Advanced triaxial testing of soil and rock*. ST 977. American Society for Testing and Materials, Philadelphia, Pa. pp. 539-552.
- Lambe, W. (1967). Stress path method. *Journal of the Soil Mechanics and Foundations Division*, 93(6), 309-331. <http://dx.doi.org/10.1061/JSFEAQ.0001058>.
- Li, P., Vanapalli, S., & Li, T. (2016). Review of collapse triggering mechanism of collapsible soils due to wetting. *Journal of Rock Mechanics and Geotechnical Engineering*, 8(2), 256-274. <http://dx.doi.org/10.1016/j.jrmge.2015.12.002>.

- Lin, B., & Cerato, A.B. (2014). Applications of SEM and ESEM in microstructural investigation of shale-weathered expansive soils along swelling-shrinkage cycles. *Engineering Geology*, 177, 66-74. <http://dx.doi.org/10.1016/j.enggeo.2014.05.006>.
- Lin, B., Cerato, A.B., Madden, A.S., & Elwood Madden, M.E. (2013). Effect of fly ash on the behavior of expansive soils: microscopic analysis. *Environmental & Engineering Geoscience*, 19(1), 85-94. <http://dx.doi.org/10.2113/gsegeosci.19.1.85>.
- Liu, X., Buzzi, O., Yuan, S., Mendes, J., & Fityus, S. (2016). Multi-scale characterization of retention and shrinkage behaviour of four Australian clayey soils. *Canadian Geotechnical Journal*, 53(5), 854-870. <http://dx.doi.org/10.1139/cgj-2015-0145>.
- Lloret, A., & Alonso, E.E. (1985). State surfaces for partially saturated soils. In *Proceedings of the 11th International Conference on Soil Mechanics and Foundation Engineering* (Vol. 2, pp. 557-562). San Francisco: CRC Press.
- Lloret, A., & Alonso, E.E., (1980). Consolidation of unsaturated soils including swelling and collapse behaviour. *Geotechnique*, 30(4), 449-477. <http://dx.doi.org/10.1680/geot.1980.30.4.449>.
- Lloret, A., Villar, M.V., Sanchez, M., Gens, A., Pintado, X., & Alonso, E.E. (2003). Mechanical behaviour of heavily compacted bentonite under high suction changes. *Geotechnique*, 53(1), 27-40. <http://dx.doi.org/10.1680/geot.2003.53.1.27>.
- Lytton, R.L. (1977). Foundations on expansive soils. *Geofisica Internacional*, 17(3), 262. [http://dx.doi.org/10.1016/0016-7061\(77\)90058-1](http://dx.doi.org/10.1016/0016-7061(77)90058-1).
- Lytton, R. L. (1977). Foundations in expansive soils. In C. S. Desai and J. T. Christian (Eds.), *Numerical Methods in Geotechnical Engineering* (pp. 427-458). New York: McGraw-Hill.
- Lytton, R.L. (1994). *Prediction of movement in expansive clays* (Geotechnical Special Publication, Vol. 2, No. 40, pp. 1827-1845). Reston: ASCE.
- Marinho, F.A.M., & Teixeira, P.F. (2009). The use of a high capacity tensiometer for determining the soil water retention curve. *Soils and Rocks*, 32(2), 91-96.
- Matyas, E.L., & Radhakrishna, H.S. (1968). Volume change characteristics of partially saturated soils. *Geotechnique*, 18(4), 432-448. <http://dx.doi.org/10.1680/geot.1968.18.4.432>.
- Nelson, J.D., & Miller, D.J. (1992). *Expansive soils, problems and practice in foundation and pavement engineering*. New York: Wiley Press.
- Nelson, J.D., Chao, K.C., Overton, D.D., & Nelson, E.J. (2015). *Foundation engineering for expansive soils*. New York: Wiley Press. <http://dx.doi.org/10.1002/9781118996096>.
- Nelson, J.D., Durkee, D.B., & Bonner, J.P. (1998). Prediction of free field heave using oedometer test data. In *Proceedings of the 46th Annual Geotechnical Engineering Conference*. Lawrence, KS: University of Minnesota.
- Nelson, J.D., Reichler, D.K., & Cumbers, J.M. (2006). Parameters for heave prediction by oedometer tests. In *Proceedings of the 4th International Conference on Unsaturated Soils* (pp. 951-961). Carefree: ASCE. [http://dx.doi.org/10.1061/40802\(189\)76](http://dx.doi.org/10.1061/40802(189)76).
- Noorany, I. (2017). Soil tests for prediction of one-dimensional heave and settlement of compacted fills. In *Proceedings of the 2nd Pan-American Conference on Unsaturated Soils* (pp. 90-99). Dallas: ASCE. <https://doi.org/10.1061/9780784481707.010>.
- Noorany, I., & Houston, S. (1995). Effect of oversize particles on swell and compression of compacted unsaturated soils. In *Proceedings of the Conference of the Geotechnical Engineering Division of the ASCE in Conjunction with the ASCE Convention* (pp. 107-121). San Diego: ASCE.
- Noorany, I., & Stanley, J.V. (1994). Settlement of compacted fills caused by wetting. In *Proceedings of the Vertical and Horizontal Deformations of Foundations and Embankments* (pp. 1516-1530). San Diego: ASCE.
- Olaiz, A.H. (2017). *Evaluation of testing methods for suction-volume change of natural clay soils* [Doctoral dissertation, Arizona State University]. Arizona State University's repository. Retrieved in March 11, 2021, from <http://hdl.handle.net/2286/R.I.46336>
- Overton, D.D., Chao, K.C., & Nelson, J.D. (2006). Time rate of heave prediction for expansive soils. In *GeoCongress 2006: Geotechnical Engineering in the Information Technology Age* (pp. 1-6). Atlanta: ASCE. [http://dx.doi.org/10.1061/40803\(187\)162](http://dx.doi.org/10.1061/40803(187)162).
- Pastor, M., Zienkiewicz, O.C., & Chan, A.C. (1990). Generalized plasticity and the modelling of soil behavior. *International Journal for Numerical and Analytical Methods in Geomechanics*, 14(3), 151-190. <http://dx.doi.org/10.1002/nag.1610140302>.
- Pereira, J.H.F., & Fredlund, D.G. (1997). Constitutive modeling of a meta-stable-structured compacted soil. In *Proceedings of the Symposium on Recent Developments in Soil and Pavement Mechanics* (pp. 317-326). Rio de Janeiro: Balkema.
- Picornell, M., & Lytton, R.L. (1984). Modelling the heave of a heavily loaded foundation. In *Proceedings of the 5th International Conference on Expansive Soils* (pp. 104-108). Adelaide: Institution of Engineers.
- Post Tensioning Institute – PTI. (2008). *Design and construction of post-tensioned slabs-on-ground* (3rd ed.). Phoenix: PTI.
- Pousada Presa, E. (1984). *Deformabilidad de las arcillas expansivas bajo succión controlada* [Doctoral thesis, Universidad Politécnica de Madrid]. Universidad Politécnica de Madrid's repository. Retrieved in March 11, 2021, from <http://oa.upm.es/508/>
- Rampino, C., Mancuso, C., & Vinale, F. (2000). Experimental behaviour and modelling of an unsaturated compacted soil. *Canadian Geotechnical Journal*, 37(4), 748-763. <http://dx.doi.org/10.1139/t00-004>.

- Riad, B., & Zhang, X. (2019). A close-form formulation for continuous prediction of at-rest coefficient for saturated soils. *International Journal of Geomechanics*, 19(10), 04019110. [http://dx.doi.org/10.1061/\(ASCE\)GM.1943-5622.0001491](http://dx.doi.org/10.1061/(ASCE)GM.1943-5622.0001491).
- Riad, B., & Zhang, X. (2020). Modified state surface approach to study unsaturated soil hysteresis behavior. *Transportation Research Record: Journal of the Transportation Research Board*, 2674(10), 484-498. <http://dx.doi.org/10.1177/0361198120937014>.
- Riad, B., & Zhang, X. (2021). A consistent three-dimensional elastoplastic constitutive model to study the hydro-mechanical behavior of unsaturated soils. *Transportation Research Record: Journal of the Transportation Research Board*. In press. <http://dx.doi.org/10.1177/03611981211002217>.
- Robles, J., & Elorza, F.J. (2002). A triaxial constitutive model for unsaturated soils. In L. Vulliet, L. Laloui & B. Schrefler (Eds.), *Environmental geomechanics* (pp. 207-213). Lausanne: Presses Polytechniques et Universitaires Romandes.
- Sánchez, M., Gens, A., Nascimento Guimarães, L., & Olivella, S. (2005). A double structure generalized plasticity model for expansive materials. *International Journal for Numerical and Analytical Methods in Geomechanics*, 29(8), 751-787. <http://dx.doi.org/10.1002/nag.434>.
- Sheng, D., Fredlund, D.G., & Gens, A. (2008a). A new modelling approach for unsaturated soils using independent stress variables. *Canadian Geotechnical Journal*, 45(4), 511-534. <http://dx.doi.org/10.1139/T07-112>.
- Sheng, D., Gens, A., Fredlund, D.G., & Sloan, S.W. (2008b). Unsaturated soils: from constitutive modelling to numerical algorithms. *Computers and Geotechnics*, 35(6), 810-824. <http://dx.doi.org/10.1016/j.compgeo.2008.08.011>.
- Sheng, D., Sloan, S.W., & Gens, A. (2004). A constitutive model for unsaturated soils: thermomechanical and computational aspects. *Computational Mechanics*, 33(6), 453-465. <http://dx.doi.org/10.1007/s00466-003-0545-x>.
- Sheng, D., Sloan, S.W., Gens, A., & Smith, D.W. (2003a). Finite element formulation and algorithms for unsaturated soils. Part I: theory. *International Journal for Numerical and Analytical Methods in Geomechanics*, 27(9), 745-765. <http://dx.doi.org/10.1002/nag.295>.
- Sheng, D., Smith, D.W., Sloan, S., & Gens, A. (2003b). Finite element formulation and algorithms for unsaturated soils. Part II: verification and application. *International Journal for Numerical and Analytical Methods in Geomechanics*, 27(9), 767-790. <http://dx.doi.org/10.1002/nag.296>.
- Singhal, S. (2010). *Expansive soil behavior: property measurement techniques and heave prediction methods* [Doctoral dissertation, Arizona State University]. Arizona State University's repository.
- Tamagnini, R. (2004). An extended Cam-clay model for unsaturated soils with hydraulic hysteresis. *Geotechnique*, 54(3), 223-228. <http://dx.doi.org/10.1680/geot.2004.54.3.223>.
- Thu, T.M., Rahardjo, H., & Leong, E.C. (2007). Soil-water characteristic curve and consolidation behavior for a compacted silt. *Canadian Geotechnical Journal*, 44(3), 266-275. <http://dx.doi.org/10.1139/t06-114>.
- Vanapalli, S., & Lu, L. (2012). A state-of-the art review of 1-D heave prediction methods for expansive soils. *International Journal of Geotechnical Engineering*, 6(1), 15-41. <http://dx.doi.org/10.3328/IJGE.2012.06.01.15-41>.
- Vassallo, R., Mancuso, C., & Vinale, F. (2007). Modelling the influence of stress-strain history on the initial shear stiffness of an unsaturated compacted silt. *Canadian Geotechnical Journal*, 44(4), 447-462. <https://doi.org/10.1139/t06-130>.
- Vaunat, J., Romero, E., & Jommi, C. (2000). An elastoplastic hydromechanical model for unsaturated soils. In A. Tarantino & C. Mancuso (Eds.), *Experimental evidence and theoretical approaches in unsaturated soils* (pp. 121-139). Boca Raton: CRC Press. <https://doi.org/10.1201/9781482283761-13>.
- Vilarrasa, V., Rutqvist, J., Blanco Martin, L., & Birkholzer, J. (2016). Use of a dual-structure constitutive model for predicting the long-term behavior of an expansive clay buffer in a nuclear waste repository. *International Journal of Geomechanics*, 16(6), D4015005. [http://dx.doi.org/10.1061/\(ASCE\)GM.1943-5622.0000603](http://dx.doi.org/10.1061/(ASCE)GM.1943-5622.0000603).
- Vu, H.Q., & Fredlund, D.G. (2004). The prediction of one-, two-, and three-dimensional heave in expansive soils. *Canadian Geotechnical Journal*, 41(4), 713-737. <http://dx.doi.org/10.1139/t04-023>.
- Vu, H.Q., & Fredlund, D.G. (2006). Challenges to modelling heave in expansive soils. *Canadian Geotechnical Journal*, 43(12), 1249-1272. <http://dx.doi.org/10.1139/t06-073>.
- Washington. Department of Army. (1983). *Technical manual TM5-818-7: foundations in expansive soils*. US Army.
- Washington. Department of Navy. (1971). *Soil mechanics, foundations, and earth structures - NAVFAC Design Manual DM-7*. US Navy.
- Wheeler, S.J. (1996). Inclusion of specific water volume within an elastoplastic model for unsaturated soil. *Canadian Geotechnical Journal*, 33(1), 42-57. <http://dx.doi.org/10.1139/t96-023>.
- Wheeler, S.J., & Karube, D. (1996). Constitutive modelling. In *Proceedings of the 1st International Conference on Unsaturated Soils (UNSAT)* (Vol. 3, pp. 1323-1356). Paris: Balkema.
- Wheeler, S.J., & Sivakumar, V. (1995). An elastoplastic critical state framework for unsaturated soil. *Geotechnique*, 45(1), 35-53. <http://dx.doi.org/10.1680/geot.1995.45.1.35>.
- Wheeler, S.J., Sharma, R.S., & Buisson, M.S.R. (2003). Coupling of hydraulic hysteresis and stress-strain behaviour in unsaturated soils. *Geotechnique*, 53(1), 41-54. <http://dx.doi.org/10.1680/geot.2003.53.1.41>.
- Wheeler, S.J., Gallipoli, D., & Karstunen, M. (2002). Comments on use of the Barcelona Basic Model for unsaturated

- soils. *International Journal for Numerical and Analytical Methods in Geomechanics*, 26(15), 1561–1571.
- White, J.L. (2007). Characteristics and susceptibility of collapsible soils in Colorado: results of a Statewide study. In *Proceedings of the 2006 Biennial Geotechnical Seminar (GEO-Volution)* (pp. 86-98). Denver: ASCE. [https://doi.org/10.1061/40890\(219\)6](https://doi.org/10.1061/40890(219)6).
- Wray, W.K., El-Garhy, B.M., & Youssef, A.A. (2005). Three-dimensional model for moisture and volume changes prediction in expansive soils. *Journal of Geotechnical and Geoenvironmental Engineering*, 131(3), 311-324. [http://dx.doi.org/10.1061/\(ASCE\)1090-0241\(2005\)131:3\(311\)](http://dx.doi.org/10.1061/(ASCE)1090-0241(2005)131:3(311)).
- Wray, W.K. (1995). *So your home is built on expansive soils: a discussion of how expansive soils affect buildings*. Reston, Va: Shallow Foundation Committee of the Geotechnical Division of ASCE/ American Society of Civil Engineers (ASCE).
- Zhang, X. (2005). *Consolidation theories for saturated-unsaturated soils and numerical simulation of residential buildings on expansive soils* [Doctoral thesis, Texas A&M University]. Texas A&M University's repository. Retrieved in March 11, 2021, from <https://hdl.handle.net/1969.1/2747>
- Zhang, X. (2010). Analytical solution of the barcelona basic model. In L. R. Hoyos, X. Zhang & A. J. Puppala (Eds.), *Experimental and applied modeling of unsaturated soils* (pp. 96-103). Shanghai: ASCE. [http://dx.doi.org/10.1061/41103\(376\)13](http://dx.doi.org/10.1061/41103(376)13).
- Zhang, X. (2016). Limitations of the suction controlled tests in the characterization of constitutive behavior of unsaturated soils. *International Journal for Numerical and Analytical Methods in Geomechanics*, 40(2), 269-296. <http://dx.doi.org/10.1002/nag.2401>.
- Zhang, X., & Briaud, J. (2015). Three dimensional numerical simulation of residential building on shrink–swell soils in response to climatic conditions. *International Journal for Numerical and Analytical Methods in Geomechanics*, 39(13), 1369-1409. <http://dx.doi.org/10.1002/nag.2360>.
- Zhang, X., & Lytton, R.L. (2008). Discussion of “A new modeling approach for unsaturated soils using independent stress variables”. *Canadian Geotechnical Journal*, 45(12), 1784-1787. <http://dx.doi.org/10.1139/T08-096>.
- Zhang, X., & Lytton, R.L. (2009a). Modified state-surface approach to the study of unsaturated soil behavior. Part I: basic concept. *Canadian Geotechnical Journal*, 46(5), 536-552. <http://dx.doi.org/10.1139/T08-136>.
- Zhang, X., & Lytton, R.L. (2009b). Modified state-surface approach to the study of unsaturated soil behavior. Part II: general formulation. *Canadian Geotechnical Journal*, 46(5), 553-570. <http://dx.doi.org/10.1139/T08-137>.
- Zhang, X., & Lytton, R.L. (2012). Modified state-surface approach to the study of unsaturated soil behavior. Part III: modeling of coupled hydromechanical effect. *Canadian Geotechnical Journal*, 49(1), 98-120. <http://dx.doi.org/10.1139/t11-089>.
- Zhang, X., Liu, J., & Li, P. (2010). A new method to determine the shapes of yield curves for unsaturated soils. *Journal of Geotechnical and Geoenvironmental Engineering*, 136(1), 239-247. [http://dx.doi.org/10.1061/\(ASCE\)GT.1943-5606.0000196](http://dx.doi.org/10.1061/(ASCE)GT.1943-5606.0000196).
- Zhang, X., Alonso, E.E., & Casini, F. (2016a). Explicit formulation of at-rest coefficient and its role to calibrate elasto-plastic models for unsaturated soils. *Computers and Geotechnics*, 71, 56-68. <http://dx.doi.org/10.1016/j.compgeo.2015.08.012>.
- Zhang, X., Lu, H., & Li, L. (2016b). Characterizing unsaturated soil using an oedometer equipped with a high capacity tensiometer. *Transportation Research Record: Journal of the Transportation Research Board*, 2578(1), 58-71. <http://dx.doi.org/10.3141/2578-07>.